

AD A089482

LEVEL II

②

OPTICS FOR LASER RADAR CROSS-SECTION MEASUREMENTS

William L. Wolfe
and
Mitchell C. Ruda
Optical Sciences Center
University of Arizona
Tucson, Arizona 85721

October 1979

Final Report for period
1 May 1975 through 31 July 1978
Under Contract DAAH01-75-C-0912

Approved for public release;
distribution unlimited.

Prepared for
Physical Sciences Directorate
U.S. Army Missile Research,
Development, and Engineering Laboratory
U.S. Army Missile Command
Redstone Arsenal, Alabama 35809

STIC
SEP 25 1980
C

DDC FILE COPY

80 9 22 240

UNCLASSIFIED

SECURITY CLASSIFICATION OF THIS PAGE (When Data Entered)

REPORT DOCUMENTATION PAGE		READ INSTRUCTIONS BEFORE COMPLETING FORM
1. REPORT NUMBER	2. GOVT ACCESSION NO.	3. RECIPIENT'S CATALOG NUMBER
	AD-A089482	
4. TITLE (and Subtitle)	5. TYPE OF REPORT & PERIOD COVERED	6. PERFORMING ORG. REPORT NUMBER
Optics for Laser Radar Cross-Section Measurements	Final Rpt. 1 May 1975 - 31 Jul 1978	
7. AUTHOR(s)	8. CONTRACT OR GRANT NUMBER(s)	
William L. Wolfe and Mitchell C. Ruda	DAAH01-75-C-0912	
9. PERFORMING ORGANIZATION NAME AND ADDRESS	10. PROGRAM ELEMENT, PROJECT, TASK AREA & WORK UNIT NUMBERS	
Optical Sciences Center University of Arizona Tucson, Arizona 85721		
11. CONTROLLING OFFICE NAME AND ADDRESS	12. REPORT DATE	13. NUMBER OF PAGES
U.S. Army Missile Command Redstone Arsenal, Alabama 35809	October 1979	
14. MONITORING AGENCY NAME & ADDRESS (if different from Controlling Office)	15. SECURITY CLASS. (of this report)	15a. DECLASSIFICATION/DOWNGRADING SCHEDULE
	Unclassified	
16. DISTRIBUTION STATEMENT (of this Report)		
Approved for public release; distribution unlimited		
17. DISTRIBUTION STATEMENT (of the abstract entered in Block 20, if different from Report)		
18. SUPPLEMENTARY NOTES		
19. KEY WORDS (Continue on reverse side if necessary and identify by block number)		
Optics Optical testing Laser radar		
20. ABSTRACT (Continue on reverse side if necessary and identify by block number)		
The laser radar simulator optical design is described. The profile of the mirror surfaces is described in detail. Two test arrangements for analyzing the optical system were set up. These were termed the "parent" and "system" tests. These tests and the resulting test results are discussed in the text. The parent test was simply a test of the optical system before the aspheric sections of the secondary and tertiary mirrors were cored out. The system test was a test of the finished optical components in their mounts. The results		

442821

Handwritten initials/signature

20. ABSTRACT (CONTINUED)

of these two tests indicated that (a) no appreciable change occurred in the optics due to the coring operation and (b) both the parent and system tests show that the optical system is performing within the required tolerances. Finally, a detailed step-by-step alignment procedure for the optics is given.

Accession For	
NTIS GMA&I	<input checked="" type="checkbox"/>
DDC TAB	<input type="checkbox"/>
Unannounced	<input type="checkbox"/>
Justification	<input type="checkbox"/>
By	
Director/	
Availability Codes	
Dist	Avail and/or special
A	

TABLE OF CONTENTS

	Page
1. OPTICAL SYSTEM	1
System Requirements	1
Aperture.	1
Speed	1
Field of View	1
Telecentricity.	1
Bistatic Angle.	1
Physical Dimensions	2
Scatter Properties.	2
Miscellaneous Requirements	2
Spherical Primary Mirror.	2
Separated Transmitting and Receiving Systems.	2
Optical Design.	2
General Description	2
Individual Mirrors--Surface Descriptions.	3
Separation of Transmitting and Receiving Systems.	7
Imagery Near the Primary Mirror Prime Focus	10
Pupil Mapping	10
Theoretical Performance.	12
On-Axis Performance	12
Full Field.	18
Transmitter Output Performance.	18
Tolerances	18
Requirements and Error Budget	18
Misalignment Sensitivities.	19
2. SYSTEM PERFORMANCE	21
Individual Component Tests	21
Primary Mirror.	21
Secondary Mirror	22
Tertiary Mirror	25
Parent System Test	25
Description of Test Arrangement	25
Test Results.	29
3. ALIGNMENT PROCEDURE	46
4. MECHANICAL DRAWINGS	60
APPENDIX A: ACCOS V USER'S MANUAL	63
APPENDIX B: COMPUTER REDUCTION OF 82-IN. MIRROR	80

LIST OF ILLUSTRATIONS

Figure		Page
1.1	Schematic of the Optical System.	4
1.2	MICOM Secondary and Tertiary Departures from Sphere	8
1.3	Separation of Transmitter and Receiver Optics.	9
1.4	Full-Size Spot Diagrams through Prime Focus.	11
1.5a	Beam Shape at Pupil Image.	13
1.5b	Beam Shape at Tertiary	14
1.5c	Beam Shapes of (a) and (b) Superimposed.	15
1.6	Theoretical Image Blur (Ray Fan) in Worst Case Direction.	16
1.7	Wavefront Profiles	17
2.1	Secondary Mirror Surface Profile as Determined by the Wire Test	23
2.2	Secondary Mirror	24
2.3	Tertiary Mirror Surface Profile as Determined by the Wire Test	26
2.4	Tertiary Mirror. Final Interferogram	27
2.5	Schematic of the Parent System Test.	28
2.6	Parent System Test. Foucaultgrams of 20 June 1977.	30
2.7	Wavefront Error as Determined by Out-of-Focus Knife Edge Test	31
2.8	Horizontal Image Spread Based on Out-of-Focus Knife Edge Test	32
2.9	Image of an Artificial Star.	33
2.10	Final System Test. Foucaultgrams through the Upper System (Horizontal)	36
2.11	Final System Test. Foucaultgrams through the Upper System (Vertical)	37
2.12	Transverse Wire Test of Upper System	38
2.13	Final System Test. Star Photos of the Upper System	41
2.14	Final System Test. Foucaultgrams through the Lower System (Horizontal)	42
2.15	Final System Test. Foucaultgrams through the Lower System (Vertical)	43
2.16	Final System Test. Star Photos of the Lower System	45
3.1	Vertex Locating Jig.	48
3.2	View of the Pickoff Flat and Notch in the Upper Rail	48
3.3	Alignment Telescope, Circular Hole in the Secondary/Tertiary Stand and the Periscope.	50
3.4	Tertiary Mirror and Its Mount.	50

LIST OF TABLES

Table		Page
1.1	Optical Element Parameters	5
1.2	Spacing Parameters	6
1.3	Misalignment Sensitivities of Optical System Elements.	20
2.1	Summary of Primary Surface Quality vs Wavelength.	21

CHAPTER 1

OPTICAL SYSTEM

In this chapter, the optical system and all information relating to it which may be useful for future modifications on the system are discussed in detail.

System Requirements

The basic system requirements are as follows:

Aperture

The system is to have a clear aperture of 78 in. diameter.

Speed

The speed of the system is $f/10$, giving an effective focal length of 780.0 in.

Field of View

The usable field of view is 2 arc-min full field. This is about 50 Airy disk diameters at a wavelength of 10.6 μm .

Telecentricity

In order to simulate the far field signal as closely as possible the system is designed to be telecentric in image space.

Bistatic Angle

The bistatic angle is the angle subtended between the laser output wavefront and the zero order scattered return wavefront. This angle is

to be no greater than 5 mrad.

Physical Dimensions

The system and target are to fit into a volume of 20 ft x 40 ft x 80 ft.

Scatter Properties

The total scatter cross section is to be less than 0.001 μm .

Performance

The system is to be diffraction limited at a wavelength of 2.0 μm .

Miscellaneous Requirements

As an outgrowth of the above requirements, several secondary properties became desirable. Among them:

Spherical Primary Mirror

A spherical primary mirror was chosen for ease of fabrication, and the increased probability of producing a smooth, low scatter surface. Such a mirror also allowed the transmitting and receiving systems to be separated.

Separated Transmitting and Receiving Systems

Scattered light analysis indicated that only one surface, the primary mirror, would be common to both transmitting and receiving systems.

Optical Design

General Description

The heart of the optical system is a three-mirror, 78-in.-aperture, $f/10$ telescope. A point source is collimated to a diameter of 78 in. The target is illuminated, and the return plane wave spectrum returns through

the system and is focused back on the image plane (see Fig. 1.1).

The three concave mirrors are sections of rotationally symmetric surfaces. The primary is spherical whereas the secondary and tertiary mirrors are aspherical, being hyperboloids deformed by higher order surface polynomial terms. Through the use of two aspherics, both spherical aberration and coma can be corrected. This was necessary in order to meet the image quality requirements across the desired field of view.

Individual Mirrors--Surface Descriptions

The optical description of the three individual mirrors and their spacing is summarized in Tables 1.1 and 1.2. All mirrors were made out of the low expansion material, Cer-vit. Note that aspheric deformation coefficients are not invariant with respect to the local coordinate system. The signs of the aspheric coefficients and radius of curvature are both needed to determine the exact surface shape. For example, the radius of a surface (such as a concave mirror) can have either a plus or a minus sign associated with it. If it is plus, the surface is concave to the right and vice versa. In either case, the sign of the conic constant will be the same. A parabola, for instance, has a conic constant of 1.0 regardless of the sign of the surface radius. However, the aspheric deformation coefficients, (of the form $z = ADy^4 + AEy^6 + \dots$), always move a surface to the right for AD, AE, ... etc. positive and vice versa. Thus, a concave surface with a positive radius of curvature (concave to the right) will be flattened by a negative AD term. A concave surface with a negative radius of curvature however, will be flattened by a positive AD term. (See ACCOS V, User's Manual in Appendix A.) The aspheric

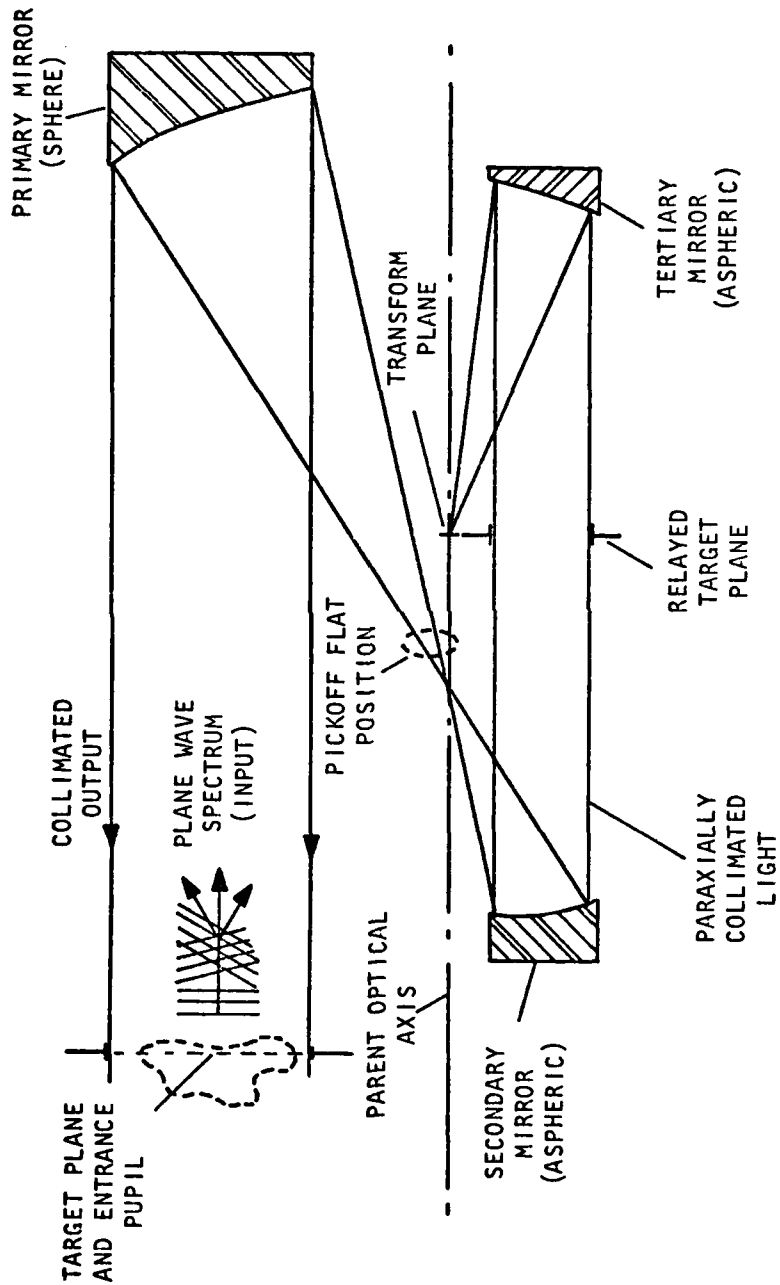


Fig. 1.1. Schematic of the Optical System.

The system is telecentric. Therefore the exit pupil is at infinity. The pickoff flat directs the return beam to another identical set of secondary and tertiary mirrors in another plane.

Table 1.1. Optical Element Parameters

<u>Element</u>	<u>Clear aperture(m)</u>	<u>Radius of curvature(m)</u>	<u>Conic & aspheric</u>	<u>h(m)</u>
Primary	78.4	-977.75	(sphere)	92.24
Secondary	9.87 (cored to 11.00)	98.79	K=-7.0484 AD=0 AE=6.622 x 10 ⁻¹⁰ AF=-1.181 x 10 ⁻¹² AG=1.1762 x 10 ⁻¹⁵	
Tertiary	8.78 (cored to 11.00)	-166.16	K=-19.385 AD=0 AE=1.801 x 10 ⁻¹⁰ AF=AG=0	

h = distance from parent optical axis to center of the section.

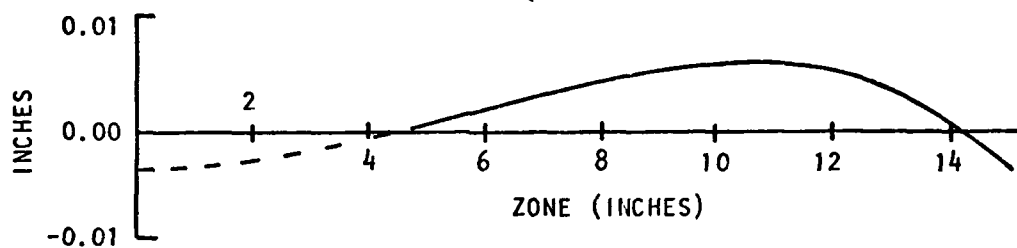
Table 1.2. Spacing Parameters. All distances are measured along the parent optical axis.

Spacing		Distance (in.)
From	To	
Target Plane	Primary	684.0
Primary	Secondary	538.270
Primary	Pickoff Flat	481.925
Secondary	Pupil Image	49.25
Secondary	Tertiary	130.462
Tertiary	Focus	83.085

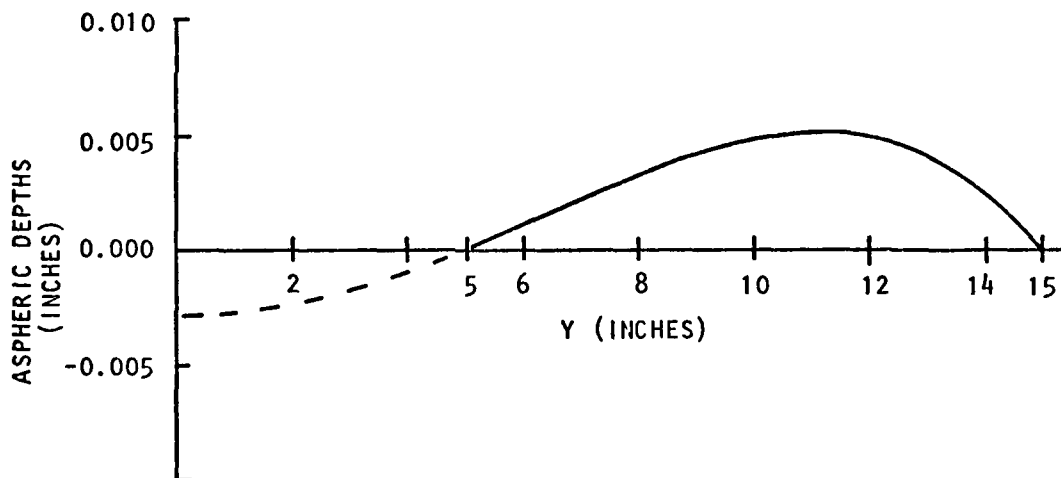
departure from a sphere of the secondary and tertiary are plotted in Figs. 1.2a, b respectively. For mechanical description of the mirrors, refer to OSC Drawing #E-2036.

Separation of Transmitting and Receiving Systems

As previously mentioned, only the primary mirror is common to both transmitting and receiving systems. This was done to reduce the total system surface backscatter. It was implemented by using the fact that a spherical mirror has no optical axis. Figure 1.3 is a schematic of the principle. We have two identical black box optical systems labeled transmitter and receiver optics. They are made to pivot about a point coincident with the center of curvature of the sphere. As a result, the images formed and the optics themselves, lie in different spaces. The imagery of the two systems, however, is identical. The only difference is that each system uses different portions of the sphere. The common union of these areas is the usable area (aperture) of the system. In our case, this area is 78 inches in diameter. Note that all focal points, final and intermediate, are separated in space. This allows for the insertion of a small flat near the focus of the primary as shown. This flat will fold one of the arms of the system causing a better physical separation of the transmitting and receiving optics. It will therefore facilitate the mechanical mounting of the components.



(a) Secondary Mirror Departure.
W/ASPH @ 0.667.



(b) Tertiary Mirror Departure.
Reference sphere radius =
173.640. Glass removal @ Y =
5 in. and 15 in. = 0.005.

Fig. 1.2. MICON Secondary and Tertiary Departures from Sphere.

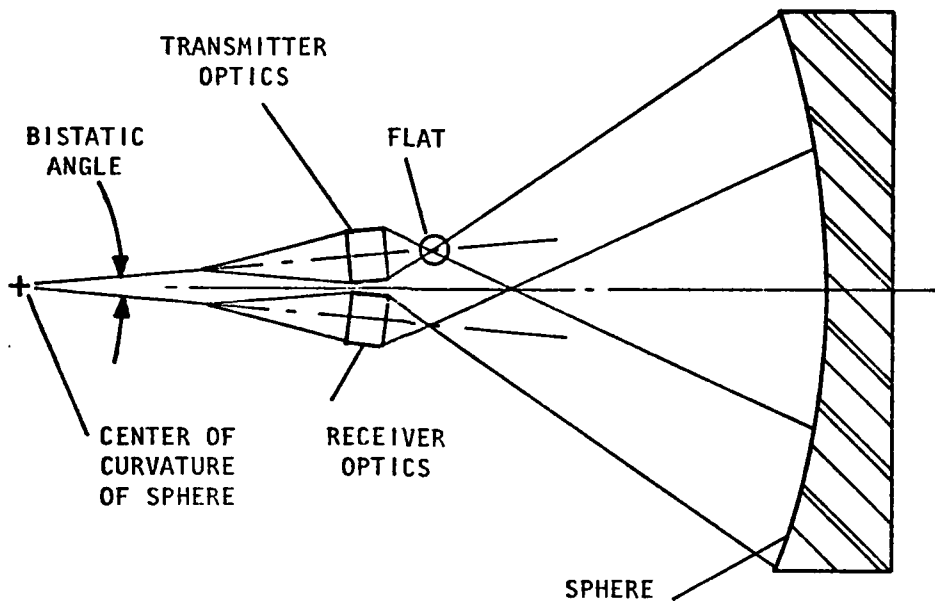


Fig. 1.3. Separation of Transmitter and Receiver Optics.

Imagery Near the Primary Mirror Prime Focus

The primary mirror generates a tremendous amount of aberration (about 1100 waves at $\lambda = 2.0 \mu\text{m}$) because it is a sphere and is used off axis. As a result, a large blur occurs instead of a sharp image at the mirror's prime focus. Figure 1.4 shows spot diagrams of the geometric blur at various focal positions near prime focus. The images shown are approximately full size. This image blur is advantageous for two reasons: First, because the image never focuses very well, air breakdown resulting from high energy densities of a 100 W laser will not be a problem. Second, since astigmatism is present in the images, there are positions (see Fig. 1.4d,h) where the images become narrow. These locations are especially suitable for picking off the beam. In this way the bistatic angle can be reduced further.

Of the two possible positions, the plane at $Z = 7.0$ in. was chosen. A pickoff mirror carefully inserted here can reduce the bistatic angle to only 1 mrad.

Pupil Mapping

Although the final image of the entrance pupil is located at infinity due to the telecentricity of the system, there is a real intermediate image of the pupil formed between the secondary and tertiary mirrors. (See drawing OSC MICOM E-0004). In an attempt to further reduce stray light effects, baffles may be placed in the pupil planes. Unfortunately, the wavefront in this region is not perfect and in fact is so aberrated that significant distortions of the entrance pupil occur. In order to insure that the baffles are correctly compensating for the distortion of the beam,

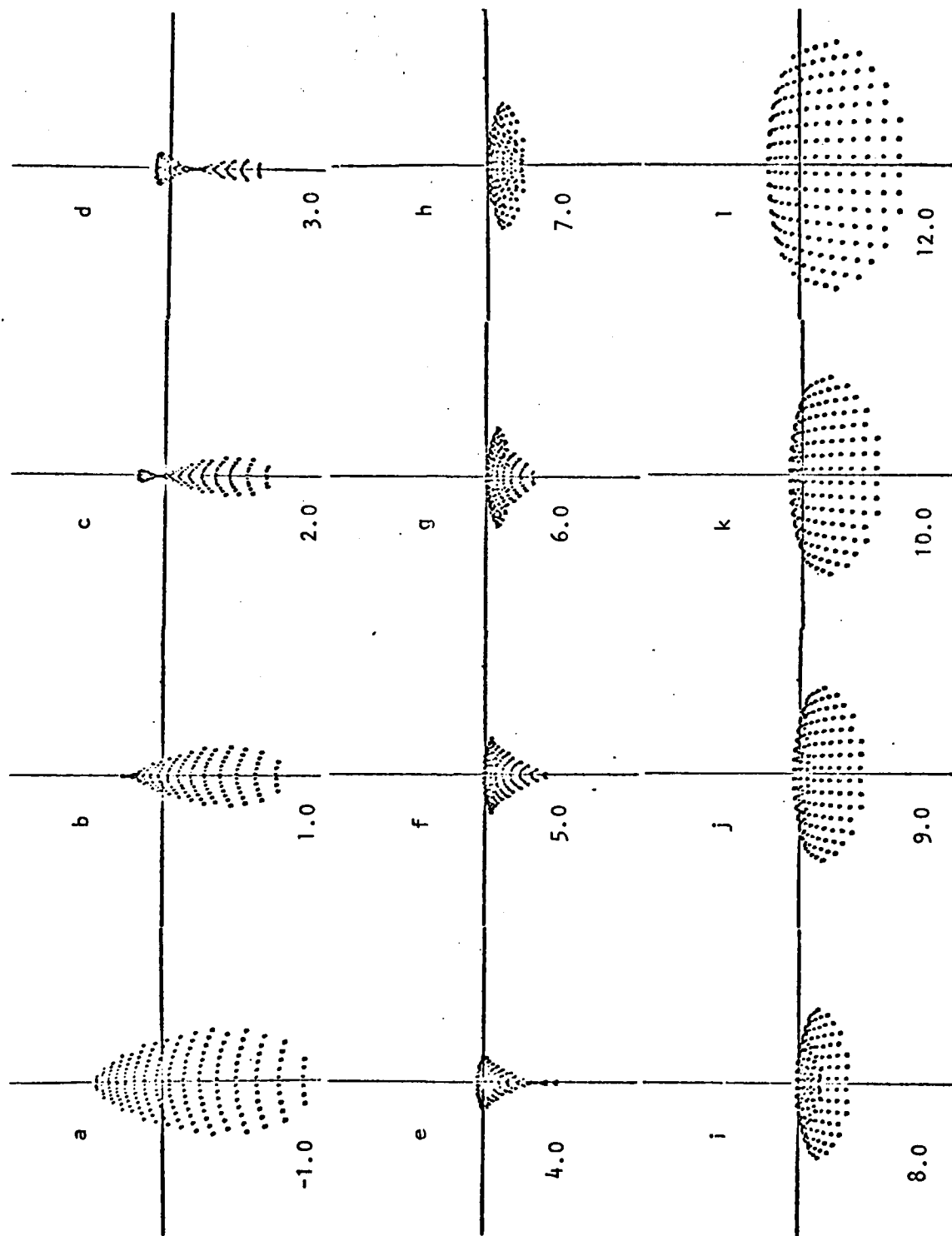


Fig. 1.4. Full-Size Spot Diagrams through Prime Focus. Numbers indicate axial position (in inches) from prime focus.

the following graphic technique can be used.

Figure 1.5 shows spot diagrams for the pupil plane, which is aberrated, and the tertiary plane, which is aberration free. A third diagram with these two planes superimposed on each other easily brings out the aberration of the pupil plane. When it is desired to make a mask, the initial shape should first be drawn out on the tertiary plane spot diagram, which is a rectangular grid of points. The diagram can then be transferred to the pupil plane grid, point for point. The resulting shape is the desired shape of the baffle, with the correct distortion taken into account.

There are two other ways of designing a baffle mask. First, since the distortion does not exceed 10%, all masks could be made 10% oversize. Another way is to place a piece of Mylar in the pupil plane. The target is then flooded with white light. A real image of the target will be seen on the Mylar. The shape of the target can be traced out on the Mylar. The pattern can then be transferred to, and cut out of, a suitable masking material.

Theoretical Performance

The theoretical performance of the system will now be discussed. The performance will be analyzed in terms of the point spread function (PSF) (Fig. 1.6) for the receiving system and the plane wavefront for the transmitting system (Fig. 1.7).

On-Axis Performance

At $\lambda = 2.0 \mu\text{m}$ the theoretical Airy disk diameter is 0.002 in. The theoretical geometric blur diameter of the optical system on axis, is

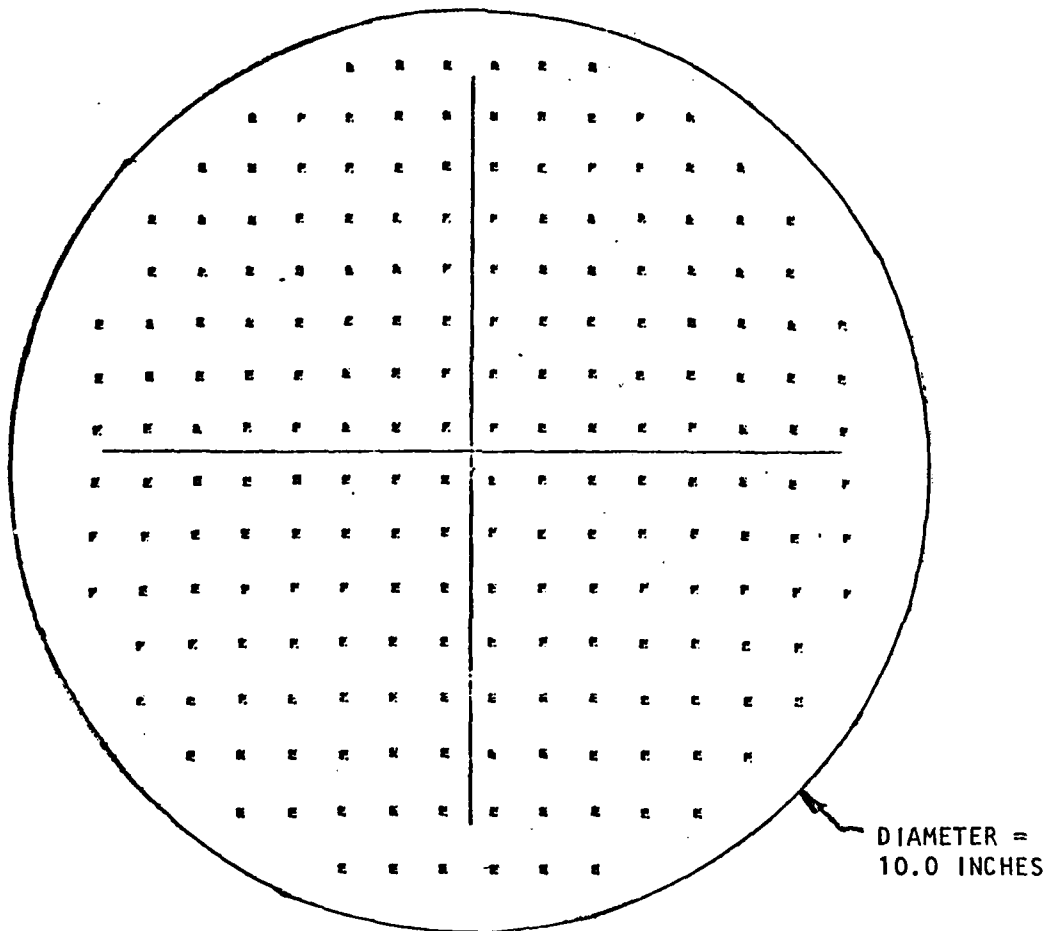


Fig. 1.5a. Beam Shape at Pupil Image.

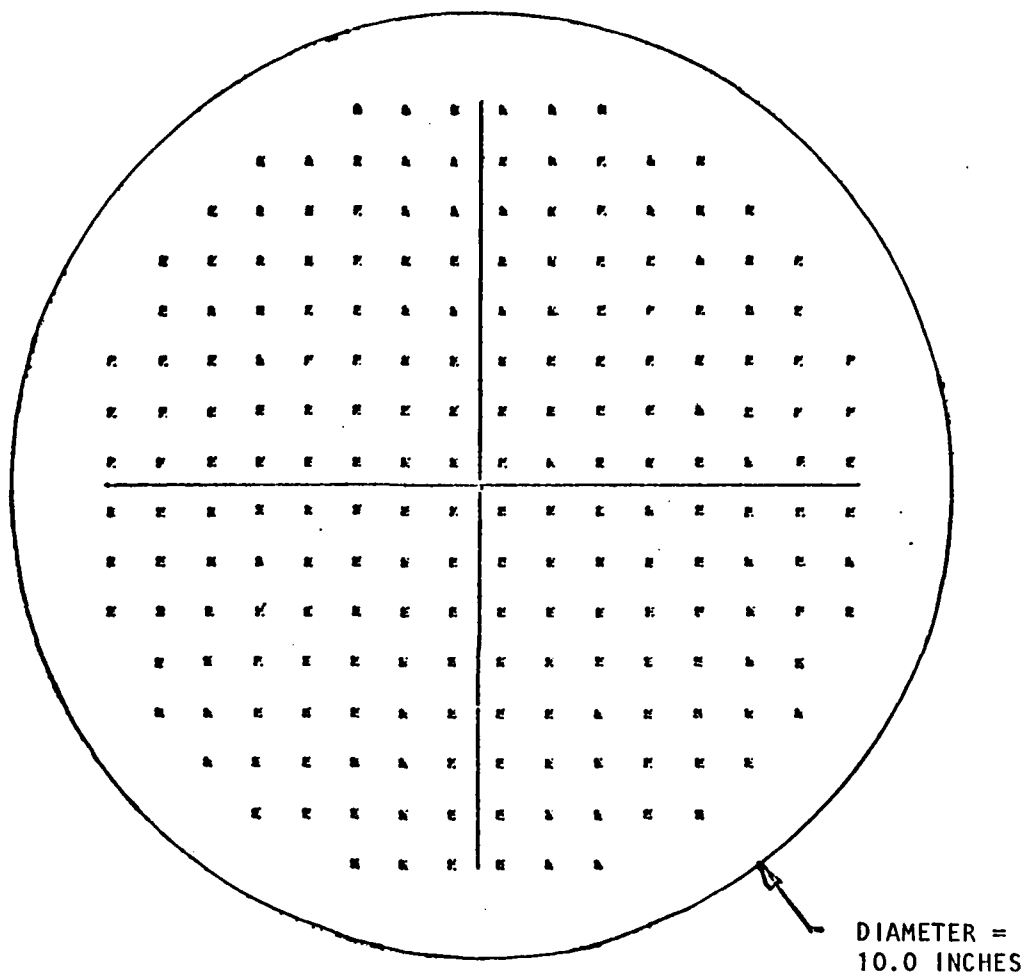


Fig. 1.5b. Beam Shape at Tertiary.

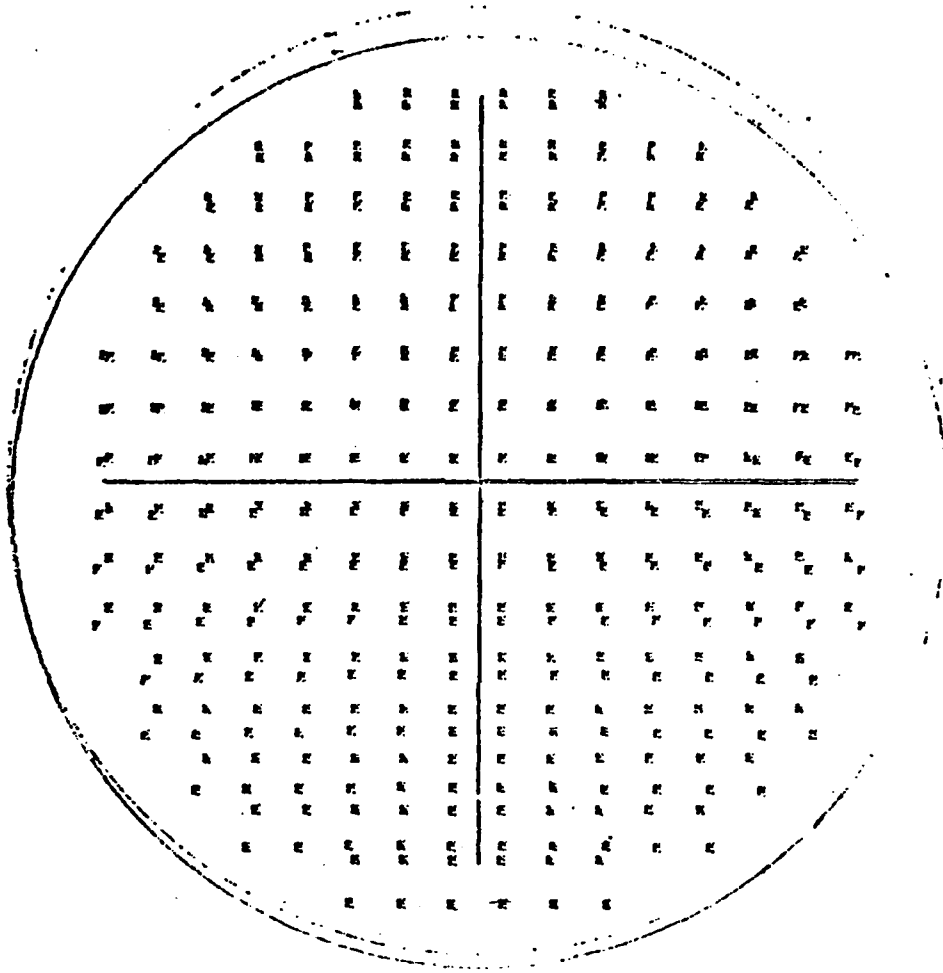


Fig. 1.5c. Beam Shapes of (a) and (b) Superimposed.

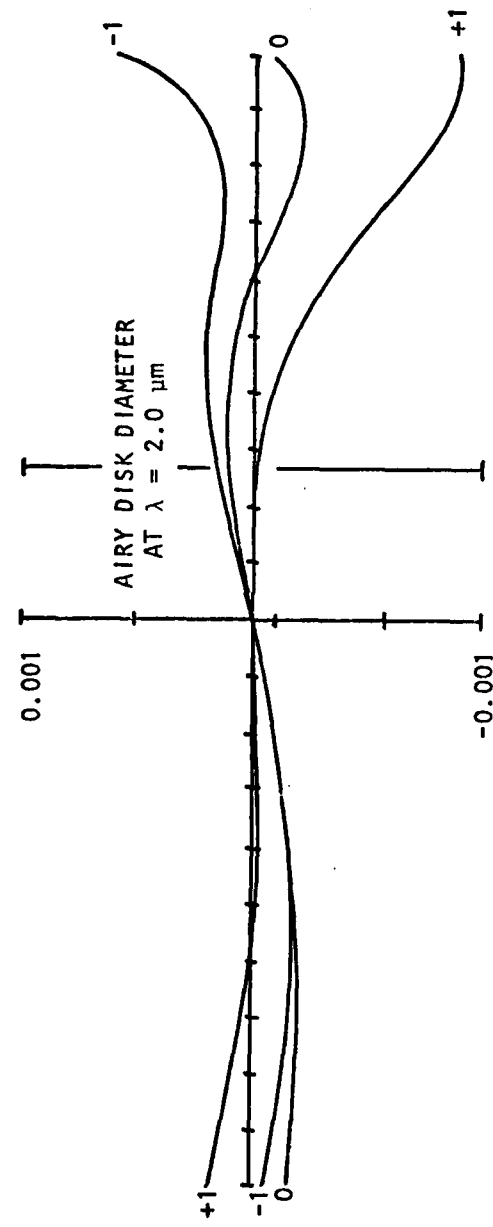


Fig. 1.6. Theoretical Image Blur (Ray Fan) in Worst Case Direction.

0: on axis. +1: upper edge of field (+1 arc min).
-1: lower edge of field (-1 arc min).

0.0003 in.--nearly an order of magnitude better than the Airy disk diameter. The corresponding peak-to-peak wavefront error is 0.085 waves.

Full Field

The geometric blur diameter at the full 1 arc-min field is about 0.001 in. The peak-to-peak wavefront error is 0.18λ (see Fig. 1.6).

Transmitter Output Performance

The performance of the transmitter and receiver arms is identical. However, it is more useful to look at wavefront phase errors in the entrance pupil plane for the transmitter since its function is to produce a collimated beam. Figure 1.7 depicts the pupil phase errors for various parts of the field. Because of the bilateral symmetry of the system, only half of the pupil phase was calculated.

Tolerances

Requirements and Error Budget

The overall performance requirement is that the system be diffraction limited at $\lambda = 2.0 \mu\text{m}$. This implies a peak-to-peak wavefront error no greater than $0.5 \mu\text{m}$ and an rms wavefront error no greater than $0.12 \mu\text{m}$. Keeping this total goal in mind, tolerances must be assigned in basically two categories: fabrication and alignment. Earlier studies showed that the alignment tolerances were relatively loose. It was also known that the mirrors would be difficult to fabricate. On the basis of these arguments, it was decided to give the bulk of the overall tolerance to the mirror fabrication.

Misalignment Sensitivities

Small misalignments of the optical system have two noticeable effects: boresight error and coma are introduced into the system. Table 1.3 lists the sensitivities of the image and wavefront errors to misalignment (tilts and decenters).

Because of the off-axis nature of the optical elements and their arrangement in space, it turns out that the most sensitive errors occur in the horizontal plane. Therefore the sensitivities will be somewhat less in the vertical plane.

Boresight error is measured in terms of angular deviation of the beam as a function of surface tilt ($\mu\text{rad}/\mu\text{rad}$) for tilts and angular deviation as a function of surface decenter ($\mu\text{rad}/\text{milli-inch}$) for decenters. Wavefront errors are measured in terms of waves/ μrad ($\lambda/\mu\text{rad}$) for tilt and waves/ milli-inch (λ/mil) for decenter. The wavefront error measured is the peak-to-peak best focused error at $\lambda = 2.0 \mu\text{m}$. The wavefront sensitivities scale inversely with wavelength.

It can be seen from Table 1.3 that misalignments of several arc-sec or several thousandths of an inch have little effect.

Table 1.3. Misalignment Sensitivities of Optical System Elements

Mirror	Tilt		Decenter	
	B ($\mu\text{rad}/\mu\text{rad}$)	C ($\lambda/\mu\text{rad}$)	B ($\mu\text{rad}/\text{mil}$)	C (λ/mil)
Primary	B	2.0	B	2.0
	C	--	C	0.038
Secondary	B	0.4	B	4.0
	C	0.009	C	0.004
Tertiary	B	0.4	B	3.2
	C	0.00025	C	-0.035

B = boresight error

C = best-focused comatic wavefront error

CHAPTER 2

SYSTEM PERFORMANCE

The system quality will now be discussed in detail. The information presented below will help in making decisions concerning which are the best areas of the wavefront. Also, it will be useful in the future if it is decided to rework any of the optical components.

In this chapter, the quality of the individual optical components (primary, secondary, and tertiary) will be discussed in detail. The results of the parent system test (that is, tests done on the system prior to coring of the off-axis sections) and final system test are presented, compared, and shown to be in good agreement.

Individual Component Tests

Primary Mirror

Interferogram. An interferogram of the 82 in. mirror was reduced on 19 February 1976. A copy of the final computer results is listed in Appendix B. A summary of the overall surface quality is listed in Table 2.1.

Table 2.1. Summary of Primary Surface Quality vs Wavelength

λ (μm)	Peak to Peak Wavefront Error (λ)	RMS Surface Error (λ)
0.6328	0.39	0.195
1.016	0.24	0.12
3.32	0.08	0.04
10.6	0.02	0.01

The conclusion reached was that at $\lambda = 3 \mu\text{m}$ or greater, the mirror performance is essentially perfect. In addition, the surface appears to be free of streaks, bubbles, etc.

Secondary Mirror

Wire Tests. The final wire tests of the parent secondary mirror were performed on 15 to 16 August 1977. These were made a few days before the cutting operation was to take place. Three separate sets of data were taken and averaged. The final mirror profile as determined by these tests is shown in Fig. 2.1. The region of interest is between the 11 cm and 38 cm zones since this is the region from which the final sections will be cored.

The results indicate that between the 11 cm and 30 cm zones, the mirror surface is good, being within $0.25 \mu\text{m}$ peak to peak ($\leq \lambda/8$ peak to peak @ $\lambda = 2.0 \mu\text{m}$) surface error. Between the 35 to 38 cm zones the peak-to-peak error is $1.75 \mu\text{m}$. The effects of this zone error will be discussed in the section on the final system test.

Interferogram. There is no final interferogram of the secondary mirror. The secondary mirror was polished and tested using the null lens and interferometer until 6 April 1976. From approximately April to August 1976, the secondary mirror was polished using knife edge data obtained from the secondary used with the other mirrors -- the so-called parent system test. Scheduling did not permit final testing of this mirror with the null lens and interferometer after reworking.

The last interferogram taken of this surface was on 6 April 1976 (see Fig 2.2). Note that this does not represent the final surface figure.

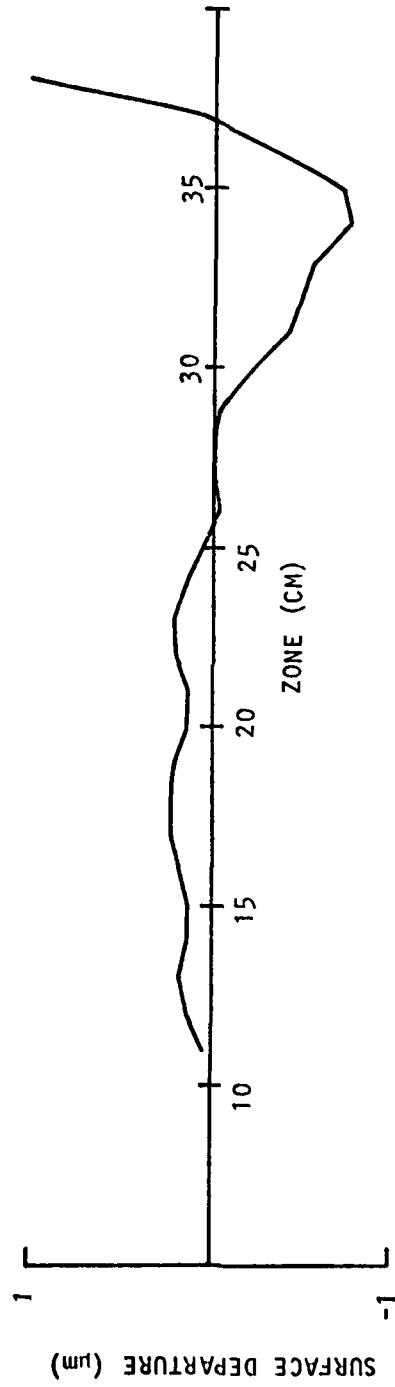


Fig. 2.1. Secondary Mirror Surface Profile as Determined by the Wire Test.

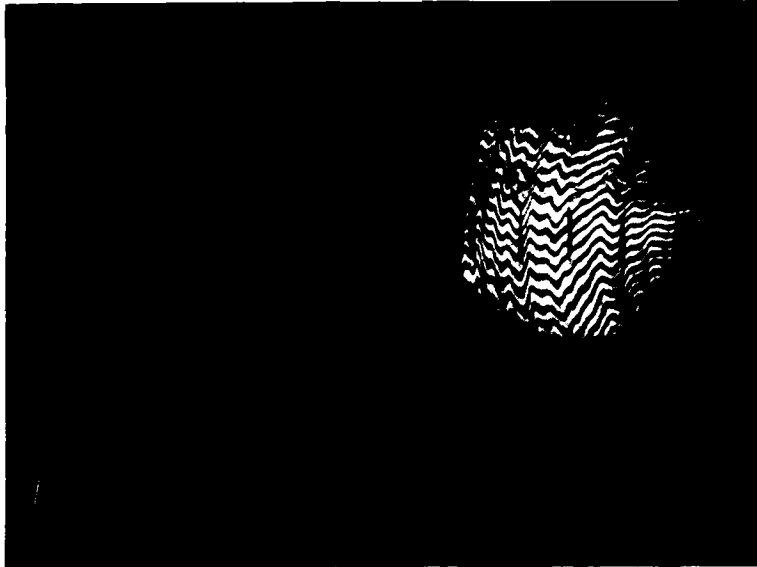


Fig. 2.2. Secondary Mirror. This represents the surface prior to polishing using the Parent system test.

Tertiary Mirror

Wire Tests. The final test of the tertiary mirror was performed on 10 May 1977. The final mirror profile as determined by these tests is shown in Fig. 2.3. The region of interest is between the 11 cm and 35 cm zones since this is the region from which the final sections will be cored.

The results indicate a generally smooth surface, 0.55 μm peak-to-peak surface error. This error is due to a single peak at the 27 cm zone.

Interferogram

A final interferogram using the null lens was taken on 9 February 1977 (see Fig. 2.4).

Parent System Test

Description of Test Arrangement

Figure 2.5 is a schematic layout of the parent-system test, a test of all three mirrors before sections are cored out. A 72-in. $f/2.7$ parabola with a 5 mW HeNe point source at its focus served as the collimator system. A white light zirconium source was also used when appropriate. The 72-in. diameter beam was, of course, unable to fill the 82-in. diameter primary mirror. Referring to Figures 2.1 and 2.3, we see that there is little reason for concern about the inner zones of the secondary and tertiary mirrors. The outer zones, however (27 to 38 cm zones) show steep departures from the nominal surface. Thus the collimator was positioned to fill the outer portions of the optical system, giving "worst case" test arrangement.

A small folding flat is located near the prime focus of the sphere. The beam is diverted to the secondary through a 90° fold. This fold was

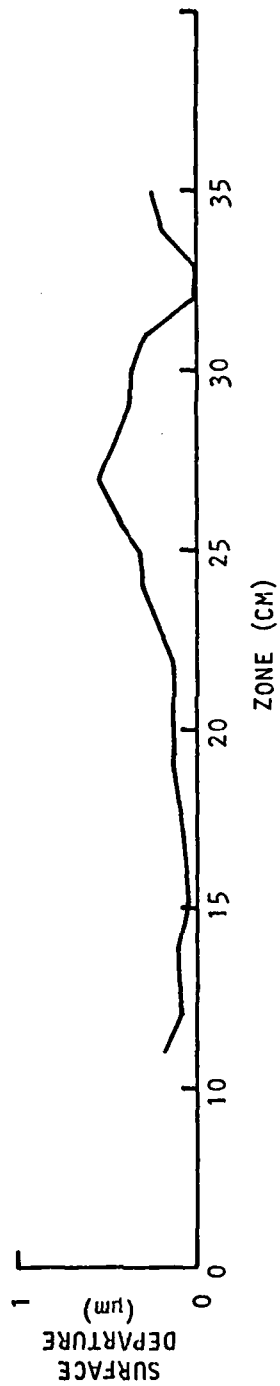


Fig. 2.3. Tertiary Mirror Surface Profile as Determined by the Wire Test.

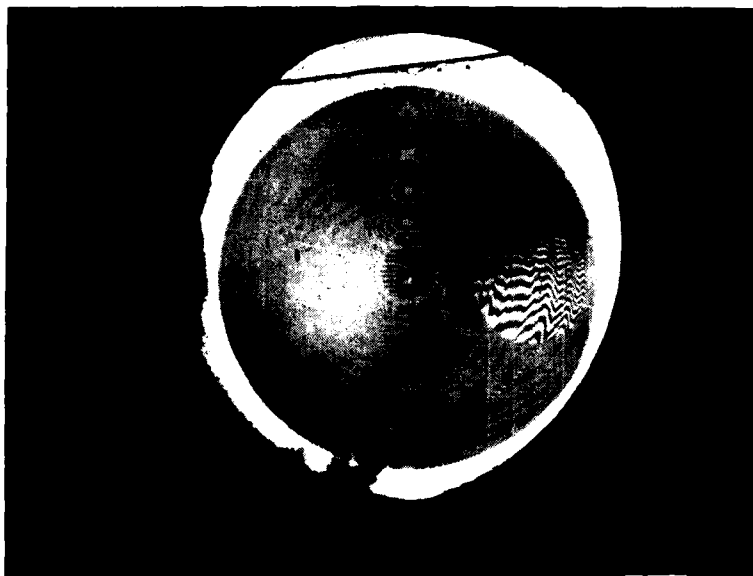


Fig. 2.4. Tertiary Mirror. Final interferogram.

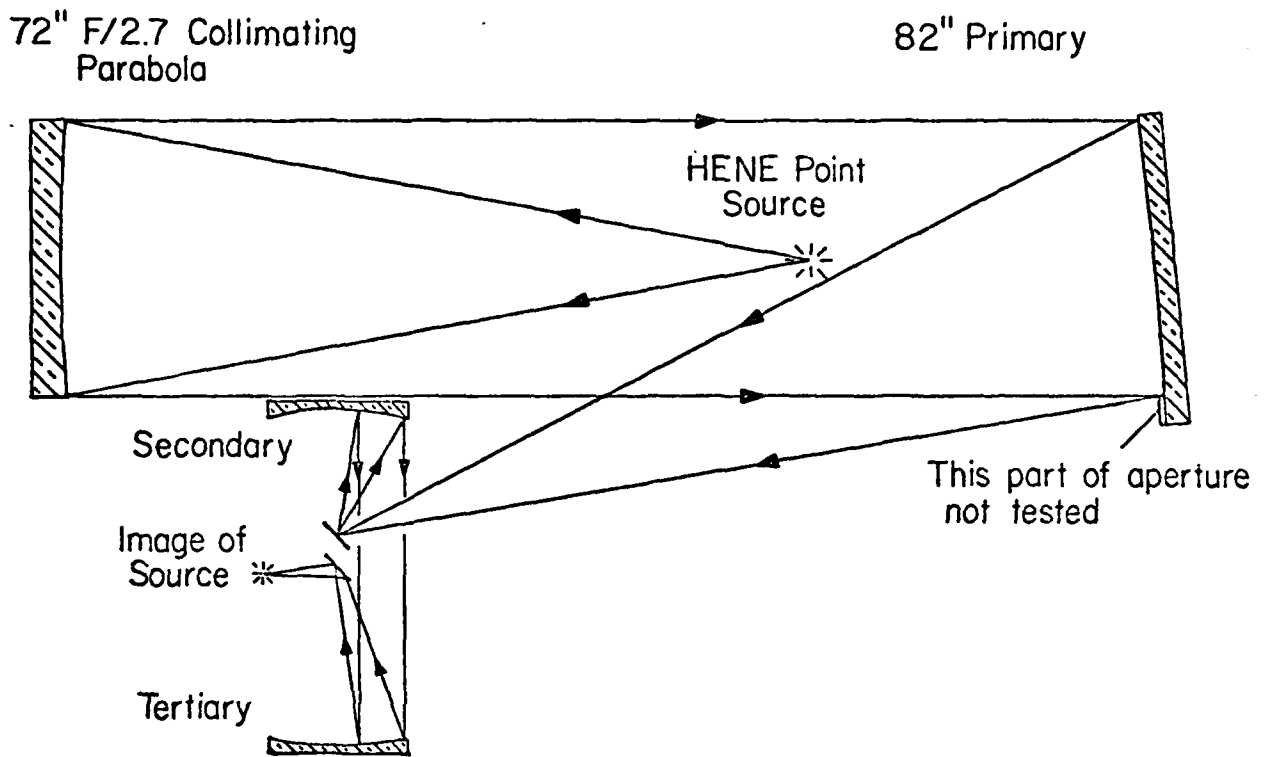


Fig. 2.5. Schematic of the Parent System Test.

necessary because without it the parent tertiary mirror would have obscured the converging beam from the primary mirror. The beam then travels to the tertiary mirror and another small folding flat.

The images of the source were then analyzed with knife edge and star tests.

Test Results

Knife Edge Photos. Knife edge photos were taken of the parent system on 29 June 1977. These photos were taken at best focus with the knife edge traveling horizontally; the knife edge itself was oriented in the vertical direction. Figure 2.6 shows a sequence of photos of the parent system wavefront as the knife edge cuts progressively further into the point spread function. The readings shown (Δx) are the knife edge travel (in inches) referenced to Fig. 2.6a.

Some general observations can be made: There are some sharp narrow zones which are cut off early by the knife edge (Figs. 2.6a,b,c). The wavefront begins cutting off most rapidly when $\Delta x = 0.0183$ in. (Fig. 2.6d). When $\Delta x = 0.220$ in. the cutoff is essentially complete. The total cutoff is 0.0037 inches. This cutoff accounts for about 73% of the wavefront area.

A more complete cutoff would be from Fig. 2.6c to Fig. 2.6g. Here the total cutoff is 0.0072 in. The amount of area cutoff is about 90%.

Transverse Knife Edge Test

Transverse knife edge tests of the parent system were performed on 4 to 5 August 1977. A total of three separate sets of data was taken and averaged. The final resulting wavefront profile of the parent system is shown in Fig. 2.7.

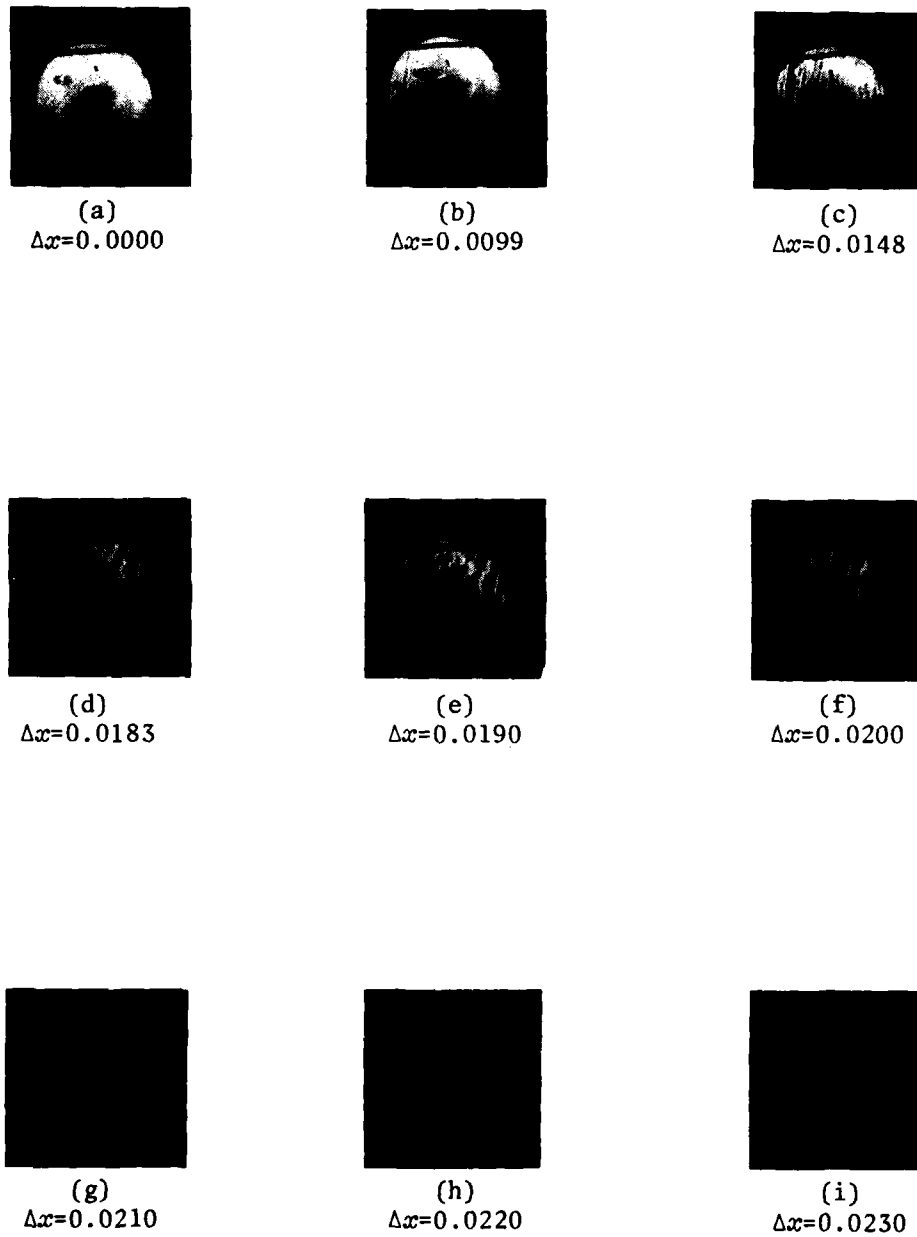


Fig. 2.6. Parent System Test. Foucaultgrams of 29 June 1977. The knife edge is cutting progressively farther into the beam. Δx is the horizontal knife edge travel in inches relative to (a).

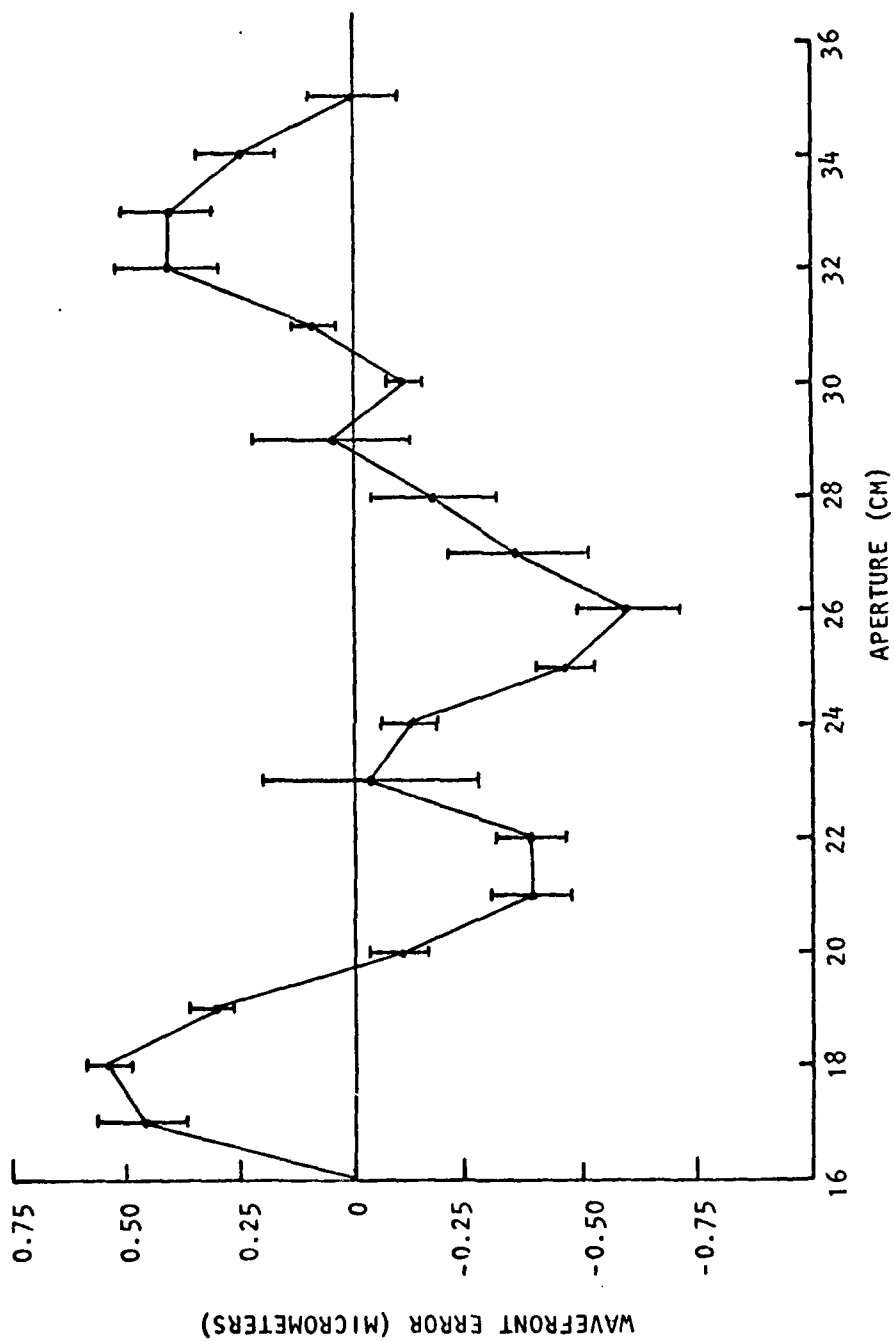


Fig. 2.7. Wavefront Error as Determined by Out-of-Focus Knife Edge Test.
(1.14 μm peak to peak).

The final peak-to-peak wavefront error is $1.14 \mu\text{m}$.

From the slope data of the transverse test, the point spread function was calculated for the horizontal direction only. Figure 2.8 is a plot of the total energy vs distance along the horizontal axis. From this analysis we find 54% of the energy within 0.0035 in. and 84% within 0.0053 in.

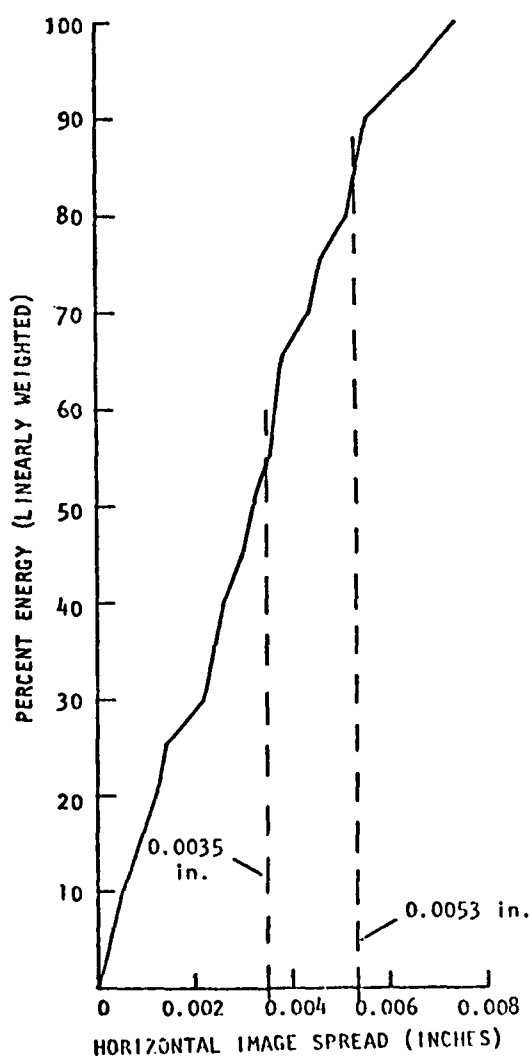


Fig. 2.8. Horizontal Image Spread Based on Out-of-Focus Knife Edge Test.

Star Photos

Images of an artificial star were photographed. These are shown in Fig. 2.9. The circle represents the desired spot size.



Fig. 2.9. Image of an Artificial Star.

Final System Test

Description of Test Arrangement. Final tests of the completed optical system were performed at the Optical Sciences Center between 15 September and 6 October 1977.

The system was tested in a single pass mode. The collimator light source and position relative to the 82 in. mirror were the same as described for the parent system test.

The primary was aluminized, the secondary and tertiary were spray silvered, and the folding flats had multilayer coatings for high reflectivity at 10.6 μm and good reflectivity in the visible.

The secondary and tertiary mirrors were cored and mounted. Wherever possible the system was aligned and set up following procedures to be used at its final site.

Various tests were performed for both the upper (receiving) and lower (transmitting) systems. These included the usual knife edge and star tests. Interferometry was not practical because of the single pass testing mode. It should be noted that these tests are more reliable and repeatable than those described in, "Parent System Test." This is primarily due to the refinements (in the mountings, their adjustments, and the alignment procedure) not available in the parent system test.

Test Results -- Upper System

Transverse Knife Edge Test. Transverse knife edge tests were performed on the optical system along two different axes. In one case the knife travels horizontally with the knife edge oriented in the vertical position.

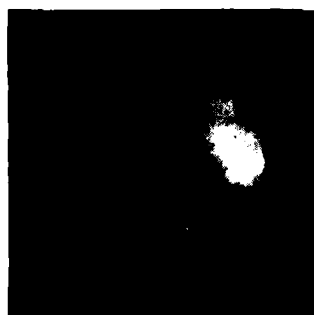
Data are taken that give slope error information. These data are then integrated to give the wavefront profile along the system's horizontal axis. In the other case, the knife travels vertically with the knife edge oriented in the horizontal position. For this test configuration no data were taken. The reason may be seen from the sequence of photos in Figs. 2.10 and 2.11. Because the cored mirror sections are rather far off axis, the zone arc segments of the parent mirror zones appear as almost vertical and parallel zones. As a result, the image blur is almost solely along the x axis. Obtaining data along the y axis was difficult, but the general statement can be made that the blur is much better in the y direction than the x direction. This will be substantiated later by total-cutoff and star-test data.

Figure 2.12 shows the final system wavefront profile. The peak-to-peak wavefront error is $1.2 \mu\text{m}$. The wavefront is within the Rayleigh criterion ($\lambda/4$ peak to peak to $\lambda = 2.0 \mu\text{m}$) for the inner 72% of the aperture.

It should be noted that, in general, the numerical integration using sample data tends to make the wavefront profile smoother than it actually is. This system is no exception.

Foucault Test. As mentioned earlier, the wavefront profile as obtained from the transverse knife edge test tends to make the surface appear smoother than it probably is. These rough portions of the wavefront can be qualitatively identified by the Foucault test. In addition, with the knife edge at the best focus image, observations of the wavefront darkening as a function of transverse knife edge cutoff into the point spread function can give useful information about the general nature and size of the spot.

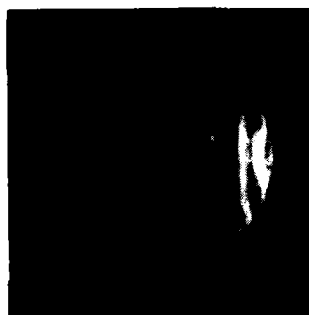
The Foucault test was performed with the knife edge positioned both



(a)
 $\Delta x = -0.0500$



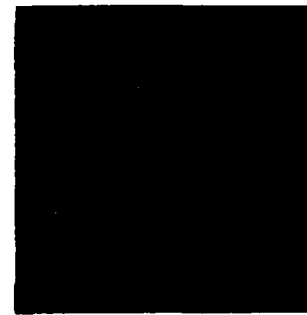
(b)
 $\Delta x = 0.000$



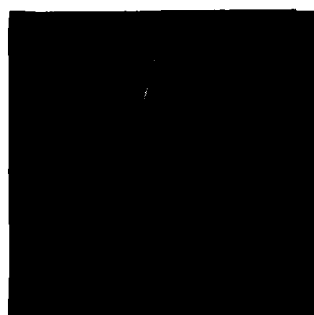
(c)
 $\Delta x = 0.0020$



(d)
 $\Delta x = 0.0040$



(e)
 $\Delta x = 0.0060$



(f)
 $\Delta x = 0.0080$



(g)
 $\Delta x = 0.0120$

Fig. 2.10. Final System Test. Foucaultgrams through the Upper System (10/8/77). The knife edge is cutting progressively farther into the beam. Δx is the horizontal knife edge travel in inches relative to (b).



(a)
 $\Delta y = 0.000$



(b)
 $\Delta y = 0.002$



(c)
 $\Delta y = 0.004$



(d)
 $\Delta y = 0.006$



(e)
 $\Delta y = 0.008$

Fig. 2.11. Final System Test. Foucaultgrams through the Upper System (10/8/77). The knife edge is cutting progressively farther into the beam. Δy is the vertical knife edge travel in inches relative to (a).

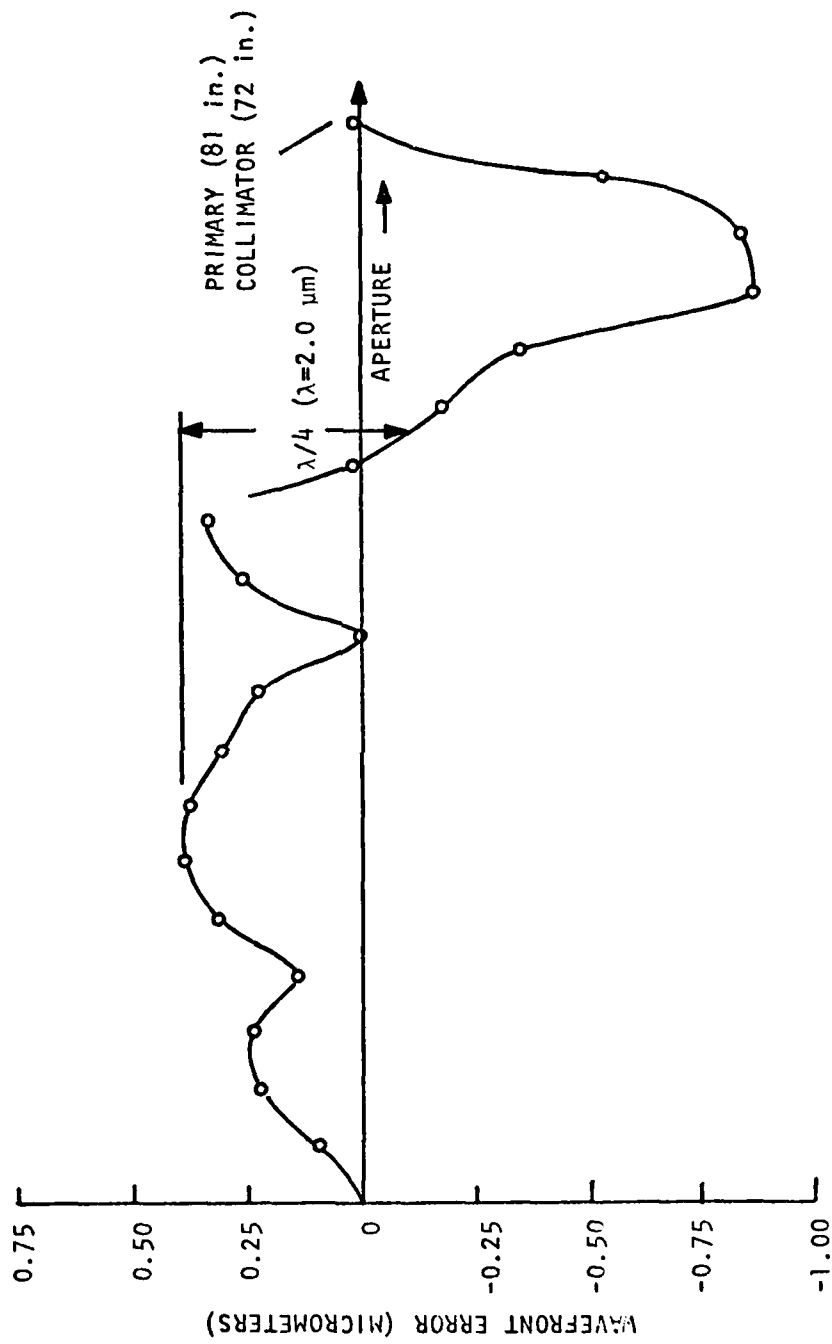


Fig. 2.12. Transverse Wire Test of Upper System. Peak-to-Peak Wavefront Error = 1.2 μm .

vertically and horizontally. Photographs of the wavefront were taken for varying knife edge positions.

Figure 2.10 shows Foucaultgrams of the upper system as the knife travels horizontally. Figure 2.11 shows Foucaultgrams as the knife travels vertically. Total travel of the knife in inches is indicated on the photographs.

We cannot determine qualitatively the image quality. Figure 2.10a shows the knife edge just beginning to block light from the outer edge of the pupil. The narrow zones appear as fine shadowed arcs. By comparison, the inner 70% of the aperture appears relatively smooth. In Fig. 2.10b the knife edge has been moved 0.050 in. Now the outer edge of the mirror is starting to darken rapidly. We use this position as our zero position. Note from Fig. 2.10b that circular as well as arc-shaped zones are visible. The circular zones are due to errors mostly on the primary mirror while some are due to errors on the collimator mirror. The arc-shaped zones are solely due to errors on the secondary and tertiary mirrors.

Figures 2.10c and 2.10d best represent the nature of the wavefront profile shown in Fig. 2.12. The surface is generally smooth over the inner 70% while showing narrow zones over the outer 30%. Between Figs. 2.10b and 2.10c the knife edge has moved 0.006 in. Approximately 80% of the energy, based on the area of the dark shadows relative to the aperture, falls within the 0.006 in. cutoff.

The sequence of photos in Fig. 2.11 shows the shadow patterns when the knife moves in the vertical direction. The zero position is shown in Fig. 2.11b. Note that circular zones are predominant. This is because, as mentioned earlier, the arc-shaped zone errors blur

the image almost exclusively in the horizontal plane. They do not affect the vertical cutoff and hence are not visible in this sequence of photographs. Again, by looking at relative areas of shadow, we find that about 90% of the energy is within 0.004 in. or between Figs. 2.11b and 2.11d.

Star Test. In the star test a microscope is used to examine the image of the point source. Figures 2.13a-c are photos of the star image. Because of the large dynamic range of the image intensity, some compromise on exposure had to be made. The exposure for Fig. 2.13a was chosen to bring out as much detail around the central core as possible without saturating the core itself. In order to get a definite image scale, a knife edge was placed on the side of the core (Fig. 2.13b). The knife edge was then moved 0.004 in. and the image was rephotographed (Fig. 2.13c).

Some general observations can be made regarding the quality of the star image: There is a central core of energy, approximately 0.004 in. or 0.006 in. in diameter, and a "flare" or "tail" extending horizontally to one side of the core. The tail is due to the zones along the outer edge of the wavefront (example: Fig. 2.10d). It is on one side of the core only because the bad zones are on one side of the wavefront only.

Test Results--Lower System

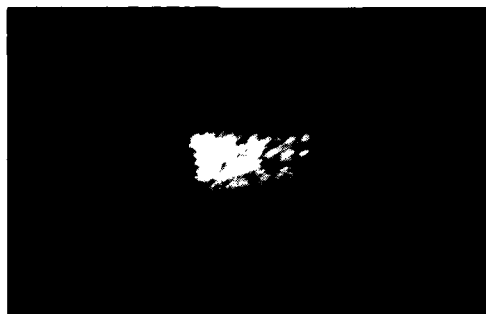
Foucault Test. For reasons discussed previously, photographs of the wavefront were taken for varying knife edge positions. Figure 2.14 shows Foucaultgrams of the lower system as the knife travels horizontally. In Fig. 2.15 the knife travels vertically. Total travel of the knife, in inches, is indicated on the photographs.



(a)



(b)



(c)

Fig. 2.13. Final System Test. Star Photos of the Upper System. (a) best-focused point spread function of the upper system. In order to determine the image scale, (b) and (c) have a knife edge (seen as a straight shadow) in the plane of the image. The knife edge travel between exposures (b) and (c) was 0.004 in.



(a)
 $\Delta x = -0.0500$



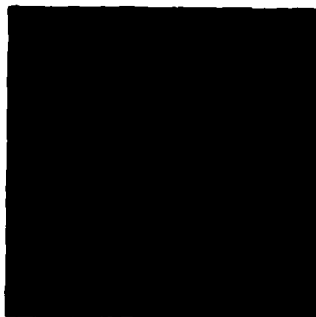
(b)
 $\Delta x = 0.0000$



(c)
 $\Delta x = 0.0020$



(d)
 $\Delta x = 0.0040$



(e)
 $\Delta x = 0.0060$



(f)
 $\Delta x = 0.0080$

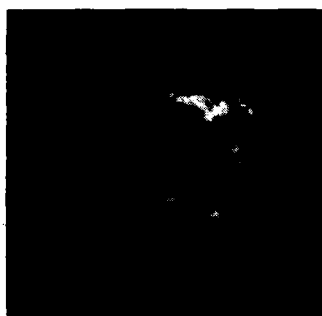
Fig. 2.14. Final System Test. Foucaultgrams through the Lower System (10/10/77). The knife edge is cutting progressively farther into the beam. Δx is the horizontal knife edge travel in inches relative to (b).



(a)
 $\Delta y = -0.0500$



(b)
 $\Delta y = 0.000$



(c)
 $\Delta y = 0.0020$



(d)
 $\Delta y = 0.0040$



(e)
 $\Delta y = 0.0060$

Fig. 2.15. Final System Test. Foucaultgrams through the Lower System (10/10/77). The knife edge is cutting progressively farther into the beam. Δy is the vertical knife edge travel in inches relative to (b).

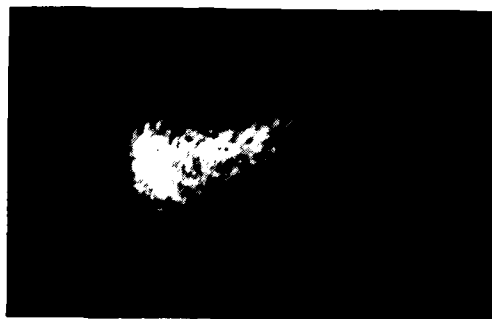
Star Test. A star test was performed on the lower system. Photos are shown in Fig. 2.16.

Comparison of Test Results

A slight misalignment of the parent test introduces aberrations. It will also map the zones on the secondary onto other than nominal positions on the tertiary. The zones in question have widths on the order of 1 cm--the same distance over which the knife edge data are averaged. Thus a slight misalignment can give different profiles. It is encouraging, however, that the average peak-to-peak and rms values remain constant.



(a)



(b)



(c)

Fig. 2.16. Final System Test. Star Photos of the Lower System. Best-focused point spread function of the upper system. In order to determine the image scale, (b) (c) have a knife edge (seen as a straight shadow) in the plane of the image. The knife edge travel between exposures (b) and (c) was 0.004 in.

CHAPTER 3

ALIGNMENT PROCEDURE

The alignment procedure consists of the following steps:

1. Attach 82-in. mirror vertex locating jig to trunnion. The center of the jig's target should be about 51.24 in. from edge of 82-in. mirror (see Fig. 3.1).
2. Locate center of curvature of 82-in. mirror. This is about 977.75 in. from jig's target. To locate this point, put a nail, pin, etc. near this point, place the eye 10 in. or more behind the pin, and look for the return inverted image of the pin. Move the pin up, down, left, and right until the tips of the pin and its real image touch. Now move your head up, down, left, and right. If the image separates from the real pin, it is because of a parallax error due to the pin not being at the proper longitudinal position. Therefore, move the pin toward or away from the 82-in. mirror until this condition is also corrected.
3. Using a suitable leveling device (optical level, theodolite, etc.), tilt the primary mirror in the vertical plane and repeat step two; keep doing this until the vertex jig target and the center of curvature of the 82-in. mirror are level.
4. Remove tilting error of 82-in. mirror in horizontal direction. This may be checked in several ways. Remember that the ultimate goal is to have the line joining the center of the 82-in. vertex jig's target and the center of the curvature parallel to and at the proper distance from the edge of the slab. Steps 2-4 are not independent; therefore,

do not try to get each step perfect before moving to the next. Rather, iterate until satisfactory alignment is achieved.

5. Move the secondary/tertiary stand into position. This is first done roughly as follows: The center of the notch (see Fig. 3.2) on the inner box beam of the upper rails (where the elliptical pick-off mirror goes) sits 6.95 in. before paraxial focus. This is best measured from the pin at center of curvature. The distance we are looking for is $977.75/2 + 6.95 = 495.83$ in. In other words, the center of the notch should be 495.83 in. from the pin defining the center of curvature of the 82-in. mirror. The feet of the secondary/tertiary stand should come to the edge of the slab.

6. Place the alignment telescope (AT) on its cones and stand as close as is reasonable to the secondary/tertiary stand. Align the AT coincident with the line between the 82-in. vertex jig and center of curvature.

7. With the AT aligned, the secondary/tertiary stand can now be aligned more precisely. The center of the circular holes in the stand marks the nominal position of the optical axis. Because of the bistatic angle and limited range of adjustment on the secondary/tertiary mounts, we want the holes off center relative to the AT. The secondary/tertiary stand should be moved closer to the edge of the slab (over if necessary) until the holes are 0.20 in. off center relative to the AT for the near hole and 0.27 in. off center for the far hole. Tolerance on these values is about ± 0.07 in. (See Fig. 3.3).

8. Now we begin alignment of the upper system. Install secondary and tertiary mirrors and mounts. Install conical vertex locating devices: the longer ones (~ 2.0 in.) go on the secondary mirror mounts, the shorter

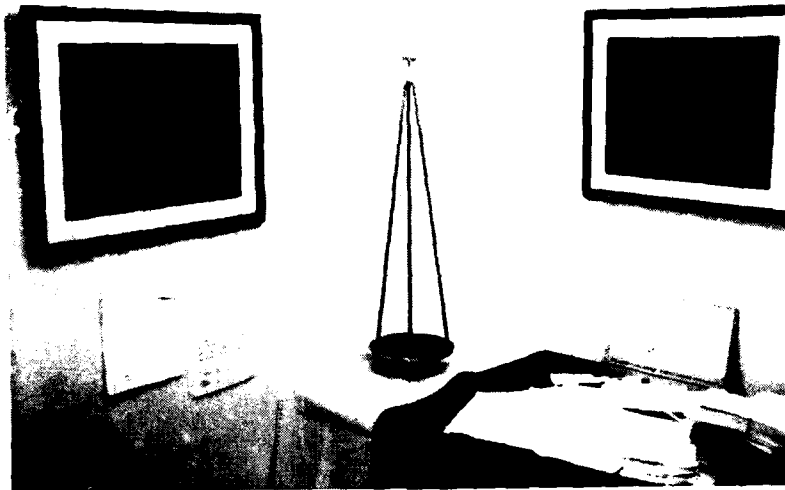


Fig. 3.1. Vertex Locating Jig.

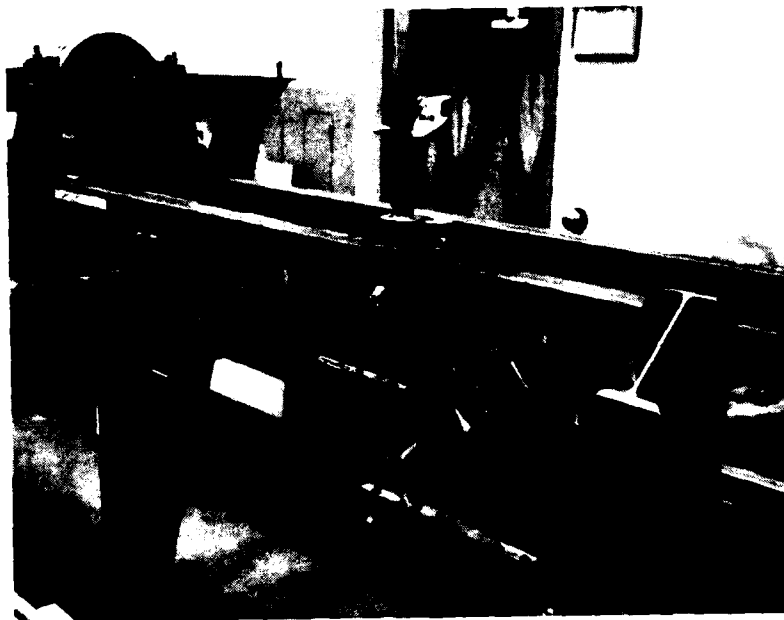


Fig. 3.2. View of the Pickoff Flat and Notch in the Upper Rail. The center of the notch should be 495.83 in. from the 82 in. mirror's vertex locating pin.

ones (~1.3 in.) go on the tertiary mirror mounts. Use spacer rod (130.46 in.) to get separation correct. (See Fig. 3.4).

9. Check alignment of AT. Remember it should be centered on pin and, when turned on the cones 180° , centered on the 82-in. vertex target. Decenter the secondary mirror (vertical and transverse to axis) until end of vertex locator is centered (vertical) and flush (horizontal) with cross hairs in the AT. If the tertiary mirror locator is in the way, remove it temporarily -- this should be done for future operations as well, if necessary. Repeat the procedure for the tertiary mirror.

Look at the vertical adjustment screws (Fig. 3.4). There are two for each mirror. When the mirrors are adjusted vertically, both screws should be adjusted simultaneously so that the trunnions are level. Look at the range of adjustment left in both the vertical and horizontal positioning screws. If they are at their maximum travel position then the lower system, when adjusted, may be out of the range of the adjustment screws. Note also that because of the effects of the bistatic angle, the lower system will be positioned 0.4 to 0.5 in. closer to the edge of the slab than the upper system. Thus the upper system should be at least 0.5 in. from the stops on the edge-of-the-slab side.

10. Now for removing tilt from the secondary mirror. Use one of the mounting plates reserved for the folding flats. Place it about 105 in. from the secondary mirror vertex. Place the interferometer mounting block on it and the interferometer on the block. With someone looking through the AT, decenter the interferometer vertically and horizontally until the point reference source is centered on the AT. Then have someone



Fig. 3.3. Alignment Telescope, Circular Hole in the Secondary/Tertiary Stand and the Periscope (Used Later for Aligning the Lower System) are Seen Here in Their Proper Positions.

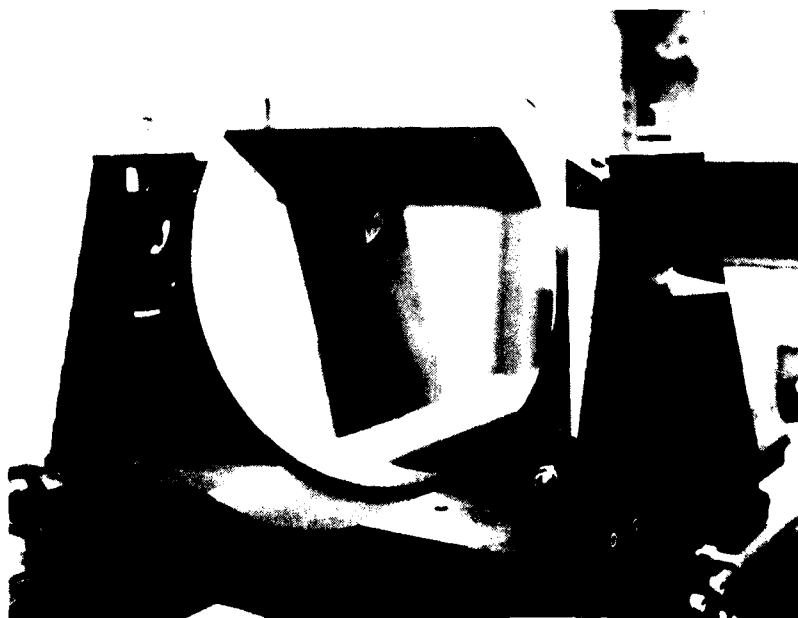


Fig. 3.4. Tertiary Mirror and Its Mount. The conical vertex locating device is shown right of center. One of the two vertical adjustment screws is located above the cone.

adjust the mirror tilt until some sort of return is seen behind the interferometer as seen in the AT. The tilt should now be small enough to refine with the wire test. Put the wire in the horizontal position, insert an eyepiece behind the interferometer, and observe the wire's shadow. If the shadow is not observable because it is at an awkward zone, repeat steps from the beginning of Step 10, changing the 105 in. distance as required. Mark this position of the rail for easy setup the next time it is required. Remove the vertical tilt by observing the shadow, rotate the wire until it is vertical, and remove the horizontal tilt. Lock all set screws and recheck.

11. To remove tilt from the tertiary mirror, remove the interferometer. Then take another mounting plate, and place it as close to the secondary mirror as possible. Place the single-axis translation stage (the one used for the elliptical mirror) on it and the post with the 6-in. mirror on top of that. Set the AT to infinity and adjust the flat until it auto-collimates off of the AT. The mirror should be to the right of the optical axis: only about 1/2 in. of the left side of the mirror should be in the field of the AT.

Measure the distance from the 6-in. mirror surface to the tertiary mirror vertex. Subtract this value from 170 in. The remainder is the approximate distance the interferometer should be placed from the flat. Place the interferometer in position and adjust the interferometer and tertiary tilt in a manner similar to the procedure for the secondary described in Step 10.

12. The next step is to get the proper distance between primary and secondary mirrors. This step may seem out of place, but the indirect

method used to adjust the spacing requires that the secondary and tertiary mirrors be reasonably aligned. If a 40 to 80-in. aperture collimator is available, it must now be set up near the target area parallel to the system optical axis and focused for infinity. At the time of this writing, this was not the case, for only a 40-in. flat was available.

The details for obtaining the correct spacing using the 40-in. will now be discussed. Place the interferometer at the back focal distance (BFD) behind the tertiary (~ 83.08 in.). Use an 83-in. spacer bar for this. With the aid of the AT, center the interferometer point source on the optical axis. Place the 40-in. flat somewhere in the 78-in. aperture near the pupil of the system. Tilt it until the return image of the point source falls back on the optical axis. Move the interferometer along the optical axis until the image falls back on the source. Measure the BFD. Note: Because the system is used off axis, the image will move left to right when the interferometer is moved. Do not worry about this effect for now. If the BFD is too short (< 83.08 in.), then move the secondary closer to the primary. Now move the tertiary to assume the 130.46 in. secondary-tertiary spacing. Next, move the interferometer until the image falls back on the source, measure the BFD and repeat the procedure until the proper BFD is obtained. Of course, if the BFD is too long (> 83.08 in.), move the secondary farther from the primary mirror.

13. With the proper mirror spacings achieved, it is desirable to repeat Steps 9, 10, and 11 to insure the alignment has not changed. Another important dimension to check is the distance from the secondary mirror vertex to the center of the notch on the upper rails. This is important

because the pickoff flat that goes there must be at the proper position in the caustic as well as at the proper position over the notch ($\pm 1/2$ in. or so). This is, of course, an over-constraint, so care must be taken in the setup procedure. The distance from the notch to the secondary mirror vertex should be 56.35 ± 0.5 in. If, after going through Steps 1 through 12, we find the secondary-to-notch spacing unacceptable, the secondary/tertiary stand must be moved an appropriate amount and the alignment procedure must be done over again. Once more, it should be emphasized that although the repetition of various parts of the alignment procedure may sound tedious, it is a "first time" only procedure.

14. The upper system is now aligned. All that remains is the alignment of the folding optics, off-axis parabola, etc. These auxiliary pieces should be aligned for the upper system before going on to the lower system.

15. The periscope must now be checked. To do this, a flat approximately 17 in. in diameter is needed. Autocollimate an AT off of the flat. (Use the AT and cones now being used for alignment of the system as they will have to be moved in the next step.) Place the periscope between the AT and the flat. Adjust the periscope so that it is approximately perpendicular to the line of sight. Now adjust the two screws that tilt one of the two folding flats on the periscope until the AT is once again autocollimated. By doing this, you have insured that the periscope is aligned (i.e., the mirrors are parallel). There is no need for the periscope to be precisely aligned; later we may find it is desirable to move it out of alignment. For now, however, we want to be nominally aligned to avoid other possible difficulties.

16. We now concentrate on alignment of the lower system. The first step is to pivot the alignment telescope about the center of curvature of the 82-in. mirror by an amount equal to the bistatic angle. For convenience, 1 mrad is a good value. Each small mark on the 82-in. vertex target jig subtends an angle of 0.2 mrad from the center of curvature. The AT should swing toward the edge of the slab (or, if you prefer, away from the 82-in. mirror). It should point toward the pin and, when reversed on the cones, point toward the leftmost hatch mark on the target.

17. With the AT in position, attach the periscope to the secondary/tertiary mount. Care should be exercised in mounting the periscope; not only is it unnecessary to clamp the periscope firmly, but doing so strains the periscope and bends it out of alignment. Look through the AT. You should be looking at the lower system. Have someone place his hand between the secondary and tertiary mirrors; focus on the hand to orient yourself.

18. Some facts about the periscope: Alignment of the periscope itself is, as previously mentioned, not critical. The basic reason for this is that in the alignment procedure that follows, the elliptical pickoff flat and the mirror that sits below it on the lower rails are aligned with the aid of two points in the lower system that have been previously defined by the AT looking through the periscope. Thus, whatever the alignment of the periscope may be, the two pickoff flats will duplicate the alignment.

Another point that should be mentioned is that periscopes are invariant under rotation and translate for collimated light only. Thus if the periscope is removed and then replaced, it probably will not return to the same position, and the lower system will appear to be out of alignment, while in fact the system may be aligned perfectly. One might then ask,

"If the lower system is aligned perfectly but, because the periscope position has changed it no longer appears aligned and I now realign the lower system to make it look aligned as viewed with the new periscope position, isn't the lower system now misaligned?" The answer is no, because included in this realignment procedure is a realignment of the pickoff flats. So, although the secondary and tertiary mirrors are in different locations, the pickoff mirrors are accounting for the change.

19. Back to the alignment procedure. The AT defines the optical axis for the lower system. Note that this axis is very close to the edge of the secondary/tertiary stand. In fact, if the periscope is either misaligned or positioned improperly, you will find yourself looking at one of the large support members of the stand. Since it is necessary to see beyond the structure, this problem must be corrected. This can be done by (a) trying to reposition the periscope or, (b) adjusting one of the periscope mirrors slightly.

20. Lower the pin that defines the center of curvature of the 82-in. mirror straight down about 16 in. or so until it is visible in the AT. Center the top on the AT crosshairs.

21. Place the secondary and tertiary mirrors in their mounts, the mounts on the rails, and the vertex finders (cones) on the mounts. The next steps are quite similar to those used in aligning the upper system.

22. Get the spacing of the mirrors correct with the 130.46 in. spacer bar. Decenter the secondary and tertiary mirrors until the vertex markers are aligned. The mirrors should be shifted along the optical axis (the direction is obvious) 16.25 in. from those of the upper system. This can be done by dropping a plumb from the vertex markers of the upper

mirror and then measuring the distance from the plumb line (horizontally) to the vertex marker of the lower mirror.

23. Now use the interferometer to remove the tilt from the secondary and tertiary in the manner it was done for the upper system.

24. Before going to the next step, make sure that as the AT is cranked through focus you see in order: (a) the tertiary vertex marker; (b) the secondary vertex marker; (c) the pin near the 82-in. mirror center of curvature (now lowered) all in proper alignment. When you have confirmed this, go on to the next step.

25. Remove the periscope. Do this by removing the two $\frac{1}{4}$ -20 screws, not by removing the single screw that interfaces the periscope to the secondary/tertiary stand. Mount the elliptical pickoff mirror and circular 6-in. folding mirror onto the rails. As a rough approximation, the center of the ellipse should be centered longitudinally over the notch in the upper rail. The same holds true for the 6-in. mirror. In the transverse direction the center of the elliptical mirror should be 0.22 in. to the right of the AT axis as seen in the AT, but centered height-wise. The 6-in. mirror should be positioned directly under the notch.

A note about the 6-in. mirror: Since its face is parallel to the support rod, it can slide along the rod without having any effect on the imaging. All that will happen is that the mirror can be centered under the notch. To change the height of the mirror above the rails at a given location, it is necessary to move the entire mirror-support structure longitudinally.

26. The flats have several degrees of freedom, thus there are several choices of adjustments to use in the alignment of the flats. Once the

user is familiar with them, he can make up his own mind. The general idea is as follows: The lower system sits 16.25 in. (nominally) below the upper system. Since the optical path (OP) for the two is identical, the lower secondary mirror must be 16.25 in. closer (longitudinally) to the 6-in. flat than the upper secondary has to be to the elliptical flat. Care was taken to separate the periscope mirrors by 16.25 in.

The elliptical and 6-in. flats also form a periscope, even though they are not rigidly attached. We must not only get the angular orientation of the two mirrors correct, but their spacing as well (16.25 in.). It is not adequate to simply measure this distance. There is another way, however. Remember that when the periscope was in position, we defined two points on the lower system optical axis. The two flats must be aligned if, when looking through the AT and off of the flats, we again see these two points on the optical axis of the AT. Now the question is simply what to adjust and by how much.

This is a good time to review the adjustments available and what they do. The elliptical mirror can be displaced vertically by sliding it on the post, translated perpendicular to the optical axis via the translation stage and moved along the optical axis by moving the entire unit along the rail (a relatively coarse adjustment).

Rotation is accomplished by two micrometers that tilt the mirror in the vertical and horizontal plane, by swinging the mirror about the axis of the support post (a coarse adjustment) and by rotating about the optical axis. This latter motion is limited by a few degrees and must be done by hand.

The only displacement available on the 6-in. flat is the coarse adjustment along the optical axis. Remember that moving the mirror along the post merely aids in centering the mirror under the notch; it does not affect the height of the optical axis!

Rotations available are the coarse rotation of the 6-in. flat about the post or the fine motion with the micrometer. The micrometer also provides tilt in the vertical plane.

27. We first align the mirrors correctly in the vertical plane. To do this, focus the AT on the pin near the 82-in. mirror's center of curvature. Tilt either mirror in the vertical plane until the pin appears at the correct height. Now focus the AT onto the secondary mirror vertex marker. Is the marker above or below the optical axis? By how much? If the marker is above the optical axis (remember that the optical axis is defined by the intersection of the crosshairs in the AT), move the entire 6-in. mirror assembly toward the pin (82-in. mirror's center of curvature) by an amount equal to the apparent displacement of the marker from the optical axis at the marker plane. Focus back on the pin and adjust the vertical tilt of one of the flats until the pin is again at the correct height. Now focus back onto the vertex marker. Is the displacement less? (It should be!) Keep iterating the procedure until you get close. Don't worry about high precision just yet.

28. We now align the mirrors in the horizontal plane. This is a little more difficult than the previous step. Tilt the elliptical mirror in the horizontal plane (with micrometer control) until the pin is centered in the AT. Now focus on the secondary mirror vertex marker. It should be in the correct vertical position but not necessarily in the correct

horizontal position. To correct this error, loosen the two set screws behind the elliptical mirror, the ones that prevent rotation of the mirror about the optical axis. Rotate the elliptical mirror. The rotation should be counterclockwise if the marker is to the right of the crosshairs and vice versa. After rotating the mirror; lock it, focus the AT on the pin and adjust the horizontal tilt as before to bring the pin back into the crosshairs. Focus back on the vertex marker. Is it closer to the crosshairs than before? Worse? Overshot? Keep iterating until the alignment is good.

29. In performing the above operation, the vertical positioning may now have to be adjusted again. Don't worry; however, this entire process converges quickly.

30. In order to move either the elliptical or 6-in. mirror longitudinally, it is necessary to loosen the mounting plates. Remember to tighten them after each longitudinal adjustment. Check at this time to make sure they are secure.

31. Are the flats secure? Look in the AT and focus on the secondary vertex marker. Is it aligned? How about the pin? Yes? Good.

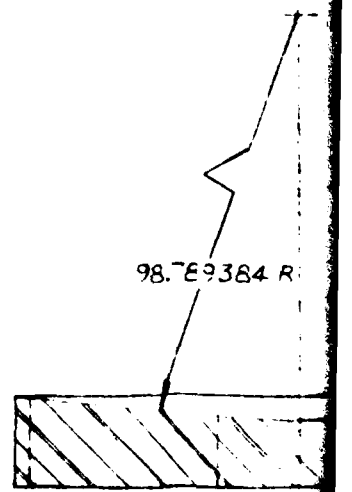
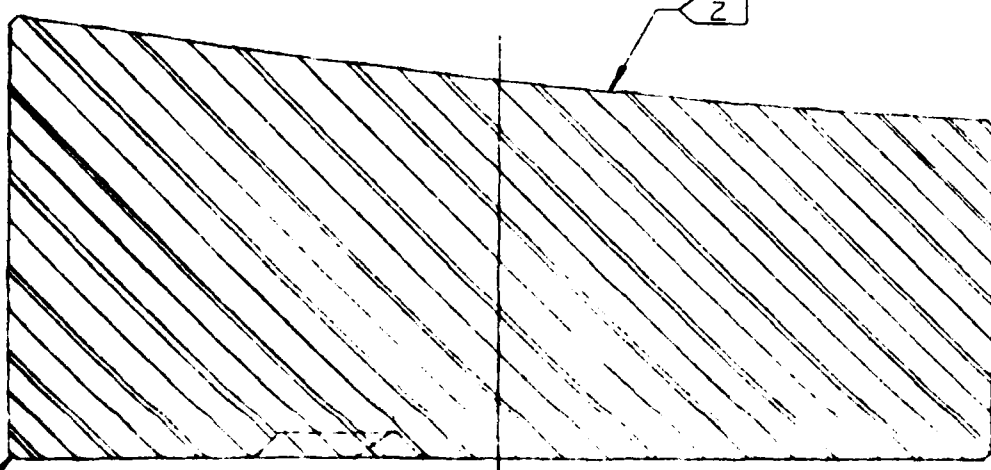
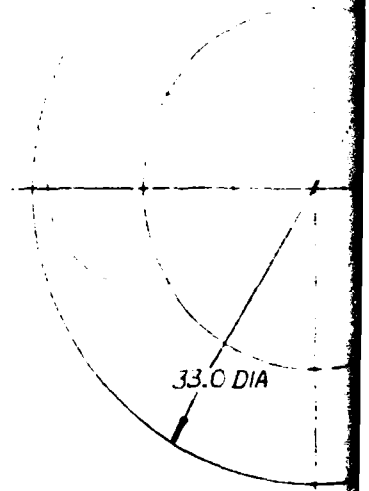
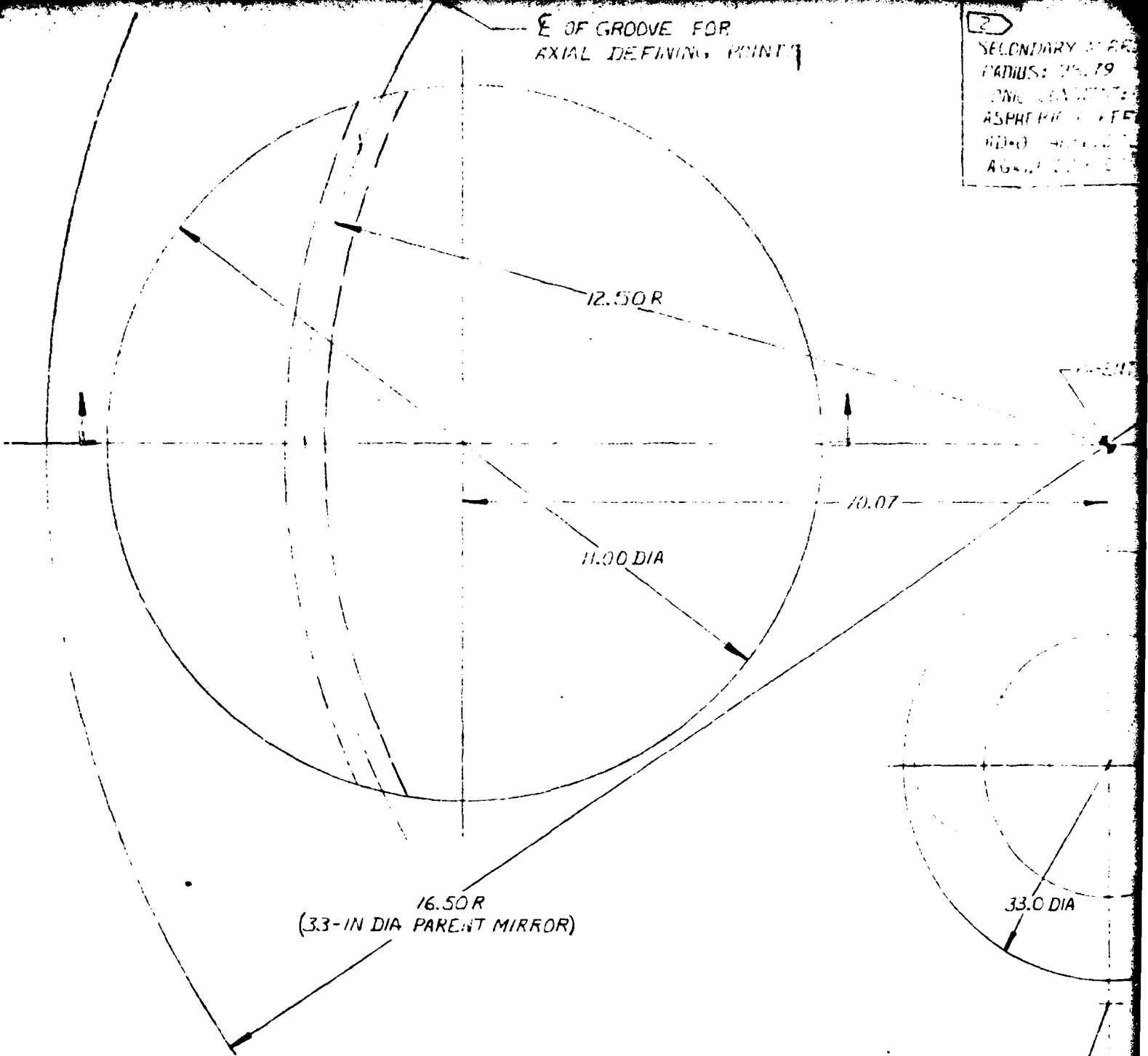
CHAPTER 4

MECHANICAL DRAWINGS

The following pages are copies of Engineering Drawings E-2036 and R-0024. Please note that the drawings have been reduced in scale.

E OF GROOVE FOR
AXIAL DEFINING POINT

2
SECONDARY MIRROR
RADIUS: 12.50 R
CONC. ELEMENT:
ASPHERIC TYPE
HD=0
AG=0.0000



.10 x 45° 2 PLACES

PARENT
SCALE

PRIMARY MIRROR - DESCRIPTION

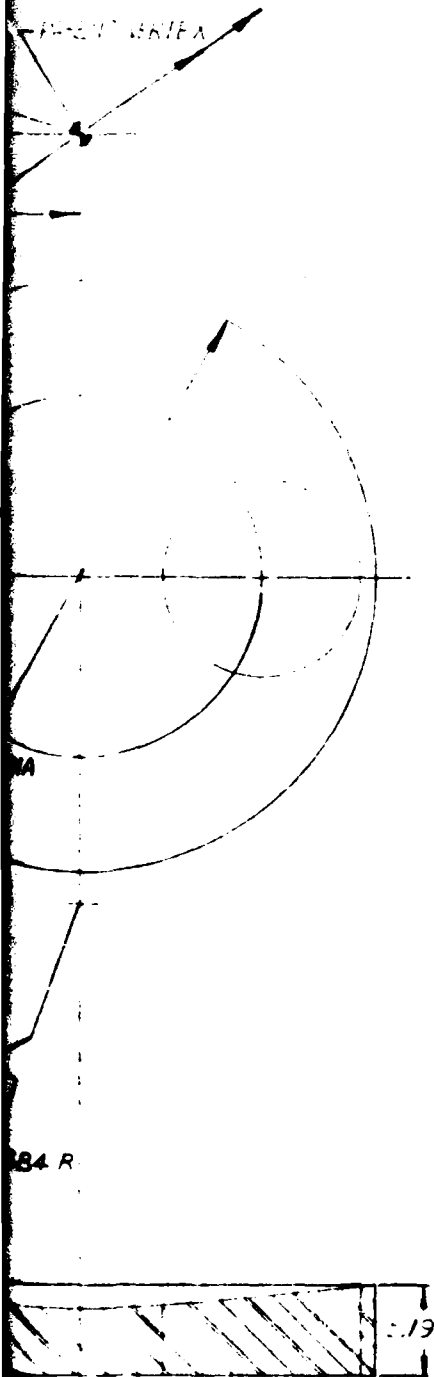
8.79
 CENTER: 1.424
 COEFFICIENTS:
 $A = 1.151 \times 10^{-10}$ $AF = -1.151 \times 10^{-12}$
 $B = 0$ $C = 0$

1

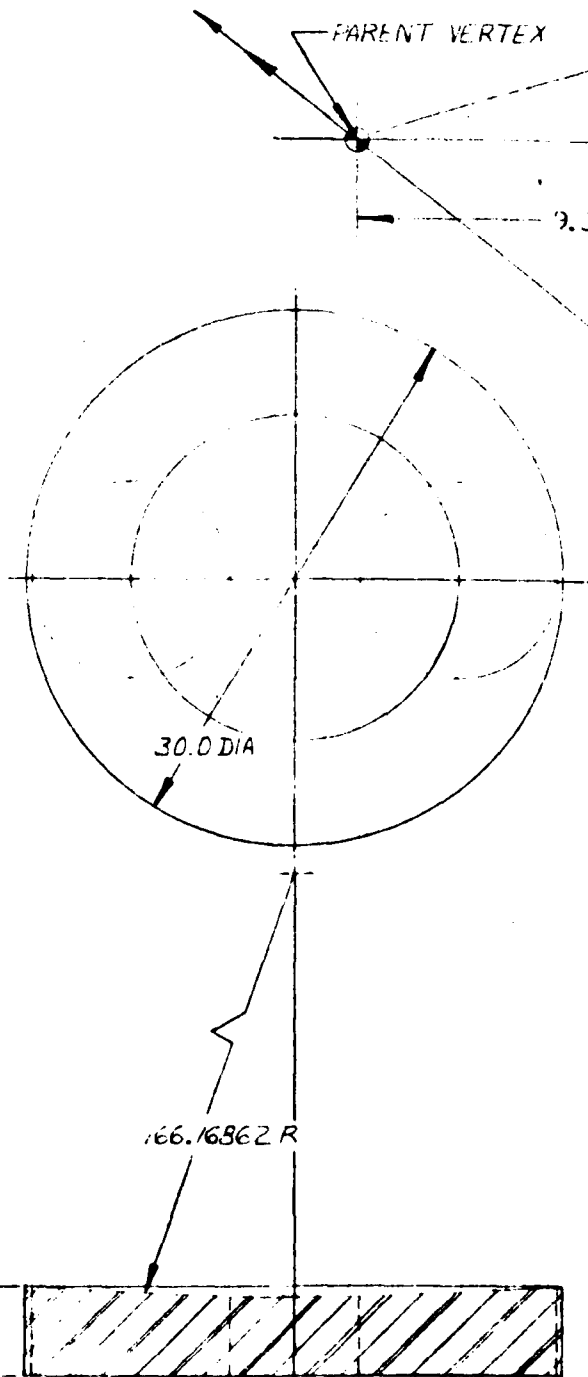
TERTIARY MIRROR PRESCRIPTION

RADIUS: -66.167
 CONIC CONSTANT: -19.584
 ASPHERIC COEFFICIENTS:
 $AD = 0$ $AE = 1.87 \times 10^{-10}$ $AF = 0$ $AG = 0$

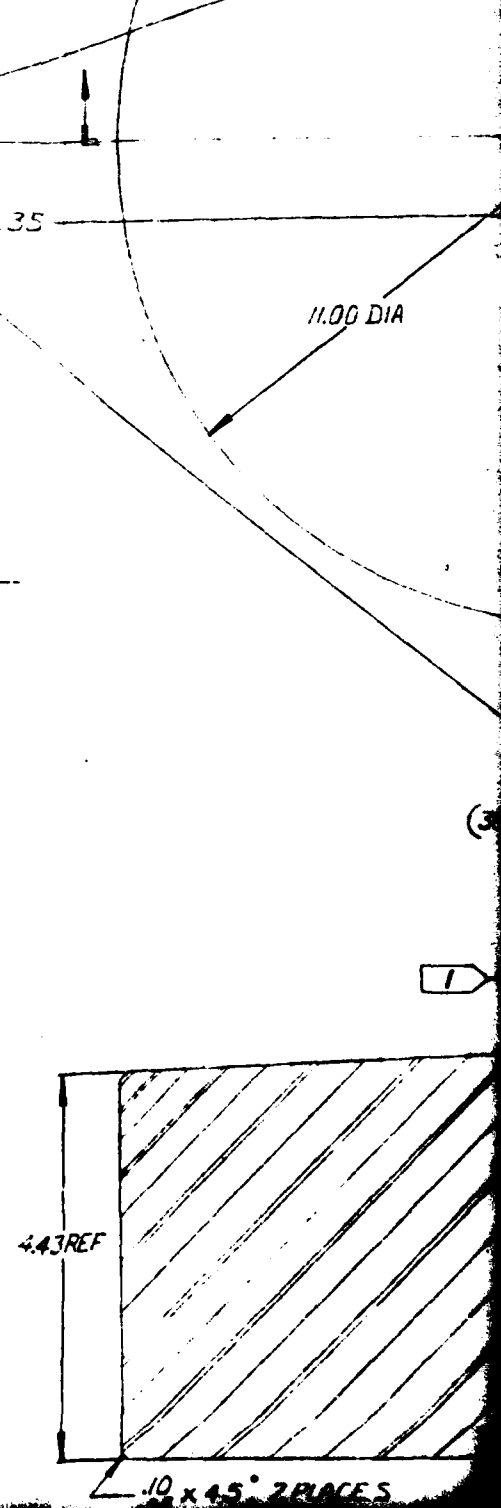
E OF GROOVE FOR AXIAL DEFINING POINTS



PRIMARY MIRROR



PRIMARY MIRROR
 SCALE = 1/5

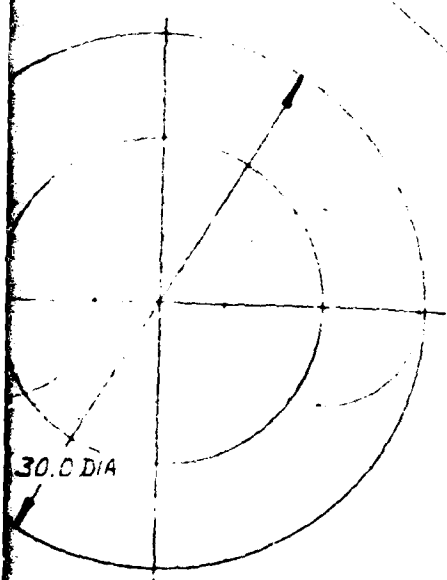
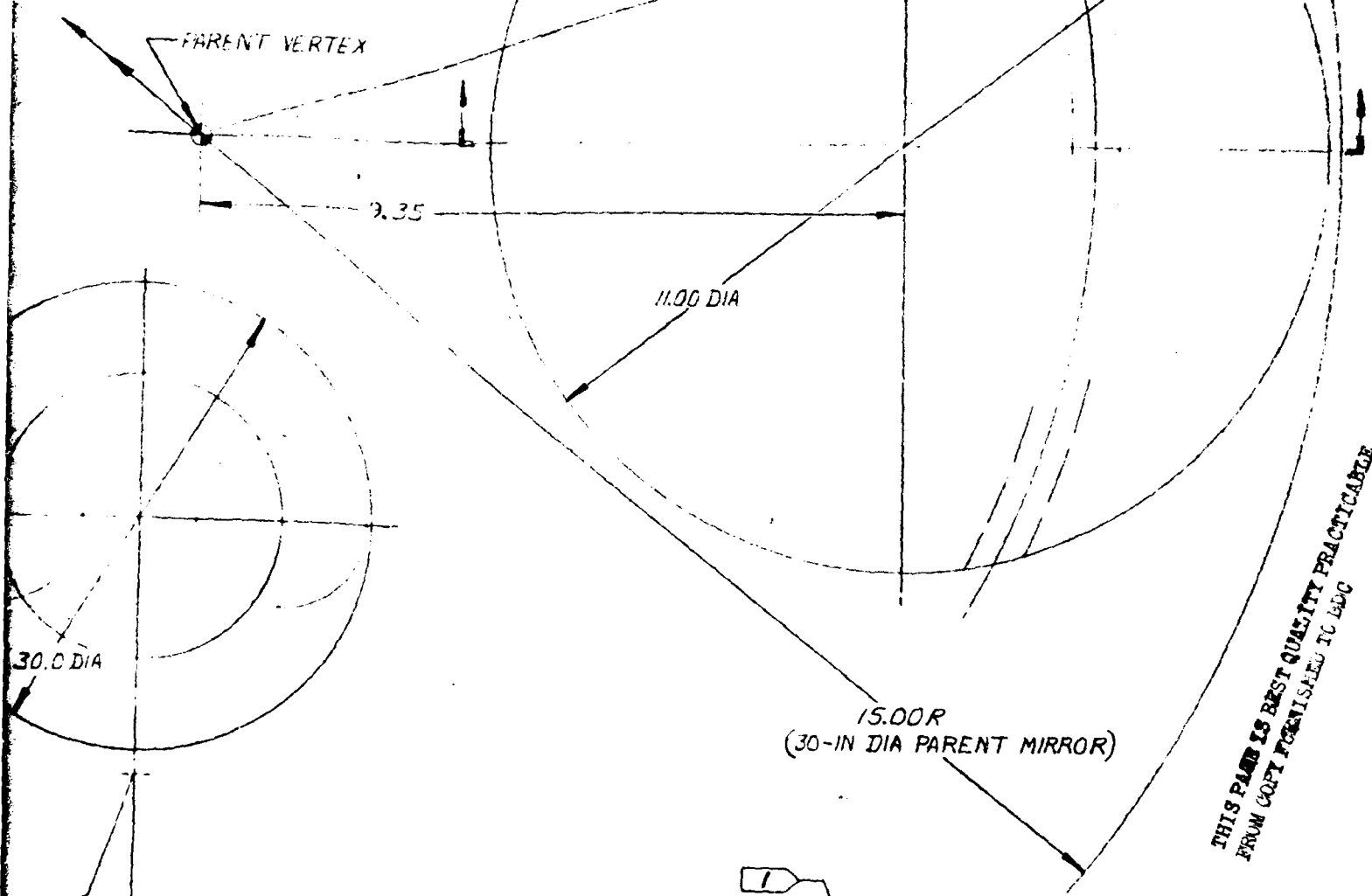


.43 REF

.10 x 45° 2 PLACES

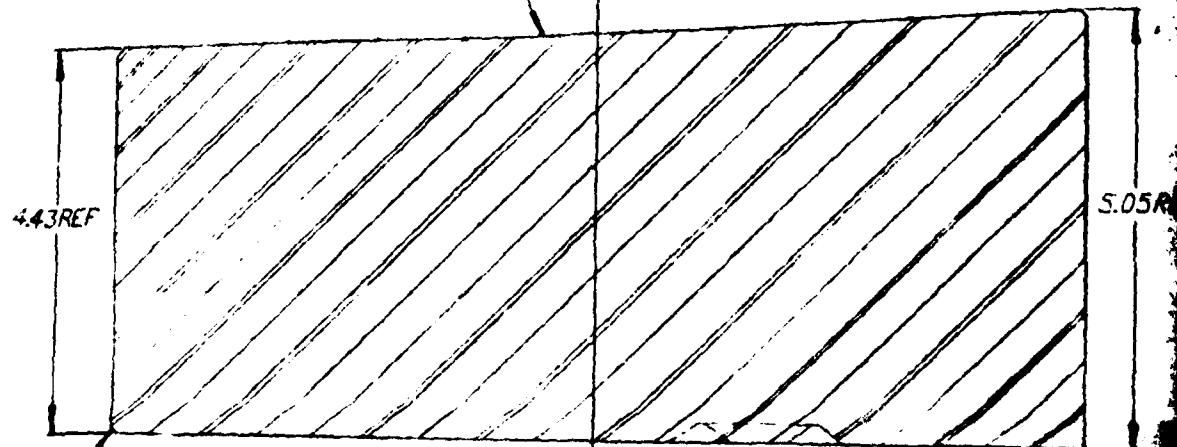
MIRROR PRESCRIPTION
 K.1.103
 INSTANT: -19.540
 COEFFICIENTS:
 E = 1.0000000000 AF = 0 AG = 0

E OF GROOVE FOR
 AXIAL DEFINING POINTS



THIS PART IS BEST QUALITY PRACTICABLE
 FROM COPY FURNISHED TO LEOC

66.16862 R

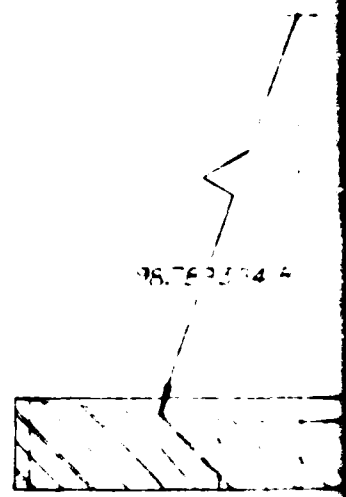
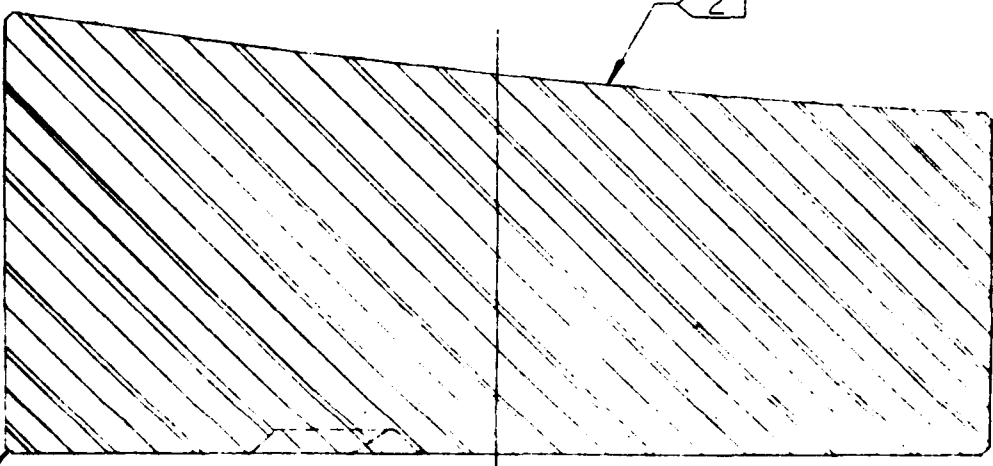


PARENT MIRROR
 SCALE = 1/5

10
 .05 x 45°, 2 PLACES

16.50R
(3.3-IN DIA PARENT MIRROR)

33.0 DIA



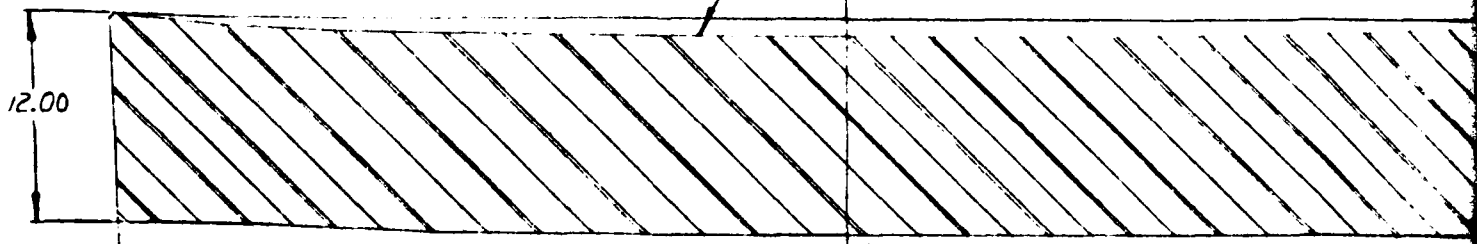
.10 x 45° 2 PLACES
.05

SECONDARY MIRROR
SCALE - FULL

PARENT MIRROR
SCALE - 1/5

977.75R

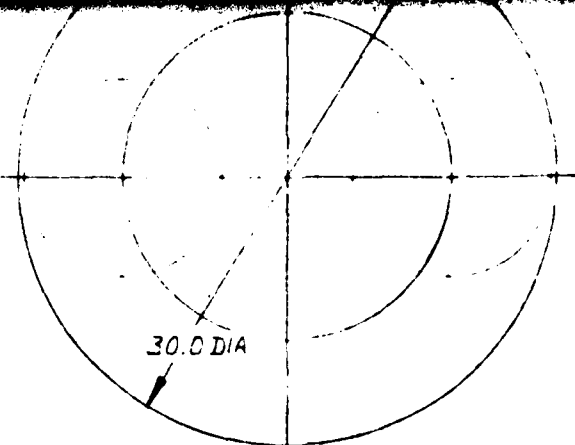
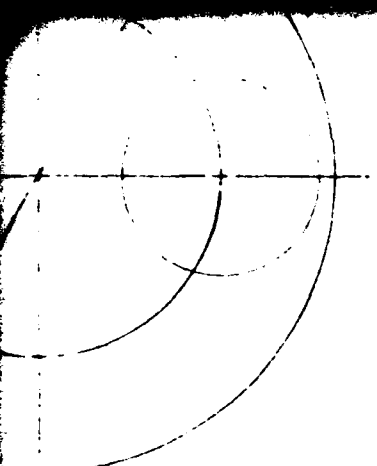
.25 x 45°
.05



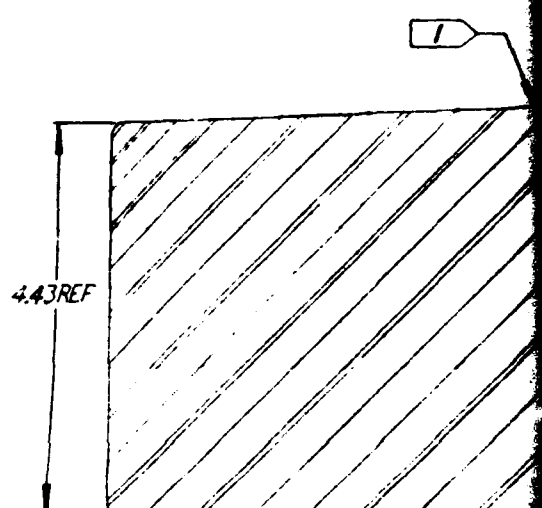
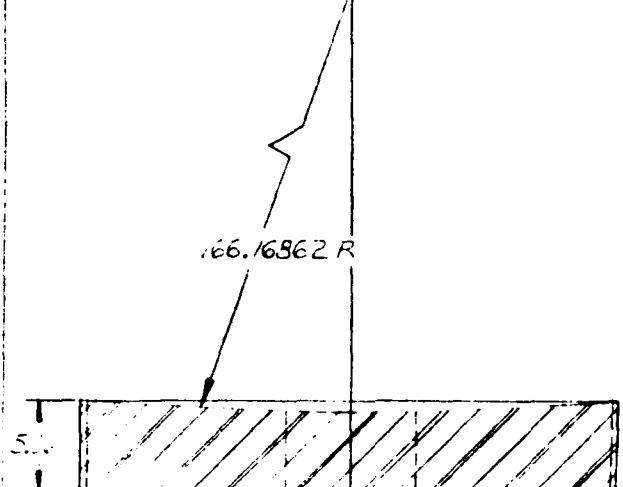
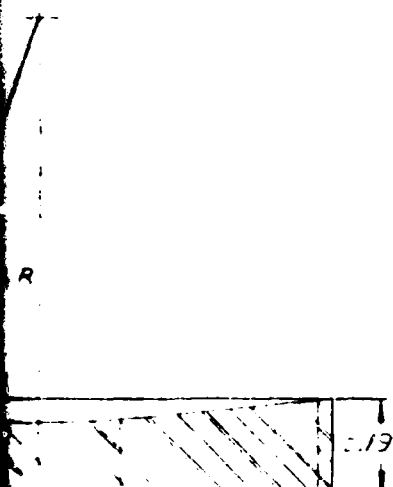
82.75 DIA

PRIMARY MIRROR
SCALE - 1/5

.50
.25



(30-1)

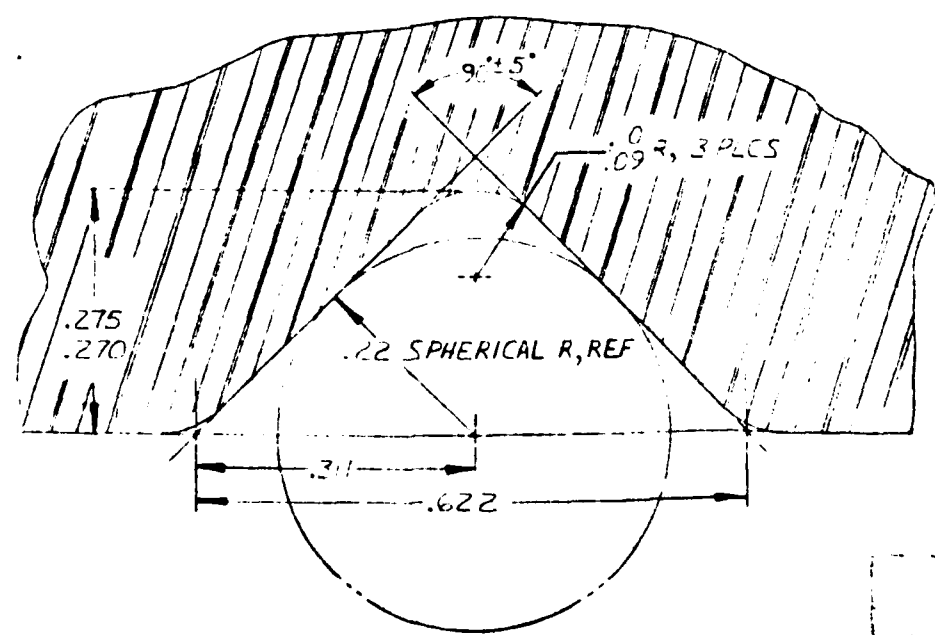
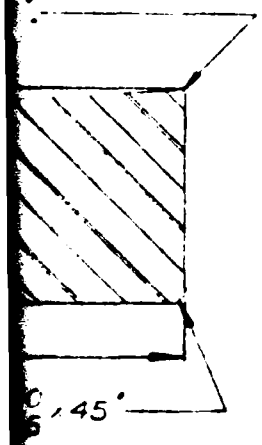


TYPICAL CROSS SECTION
SCALE = 1/5

PARENT MIRROR
SCALE = 1/5

.10 x 45°; 2 PLACES
.05

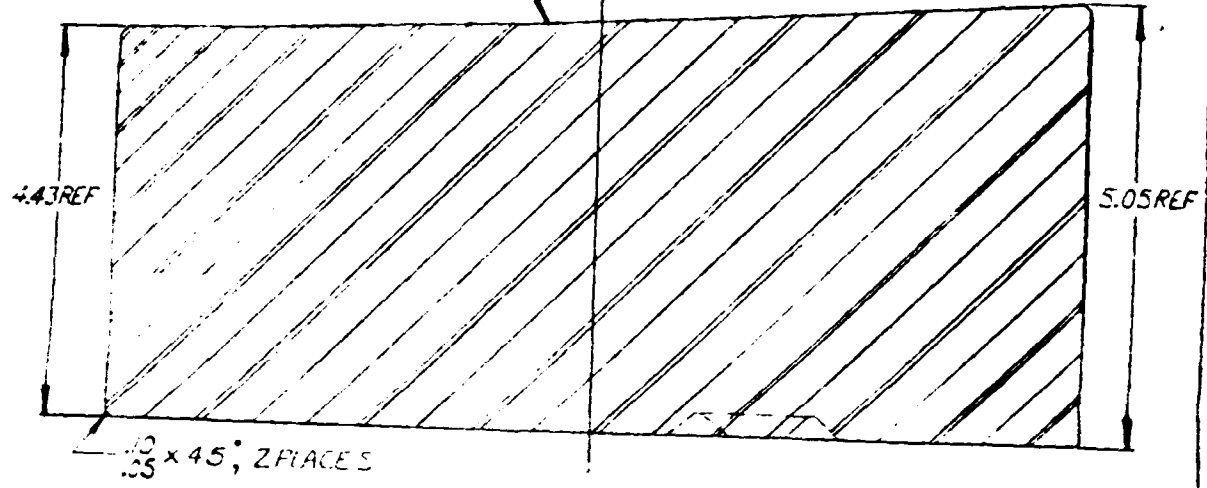
TERTIARY



TYPICAL CROSS SECTION OF GROOVES
SCALE = 10/1

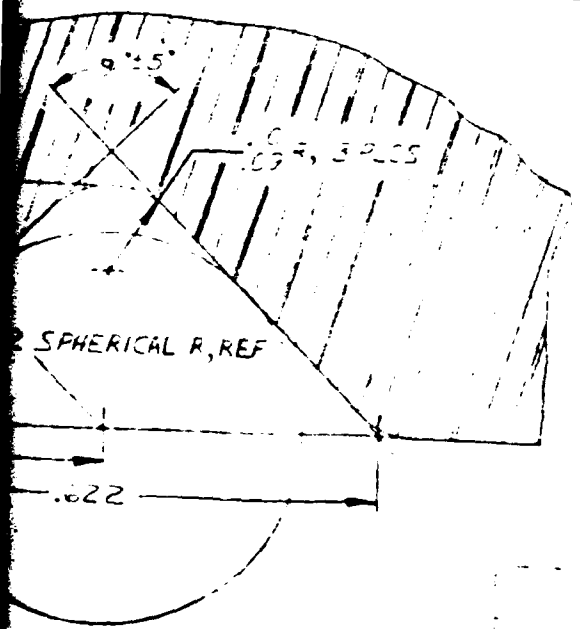
15.00R
(30-IN DIA PARENT MIRROR)

THIS PAPER IS BEST QUALITY PRACTICABLE
FROM COPY FURNISHED TO ADC



MIRROR
E-1/5

TERTIARY MIRROR
SCALE - FULL



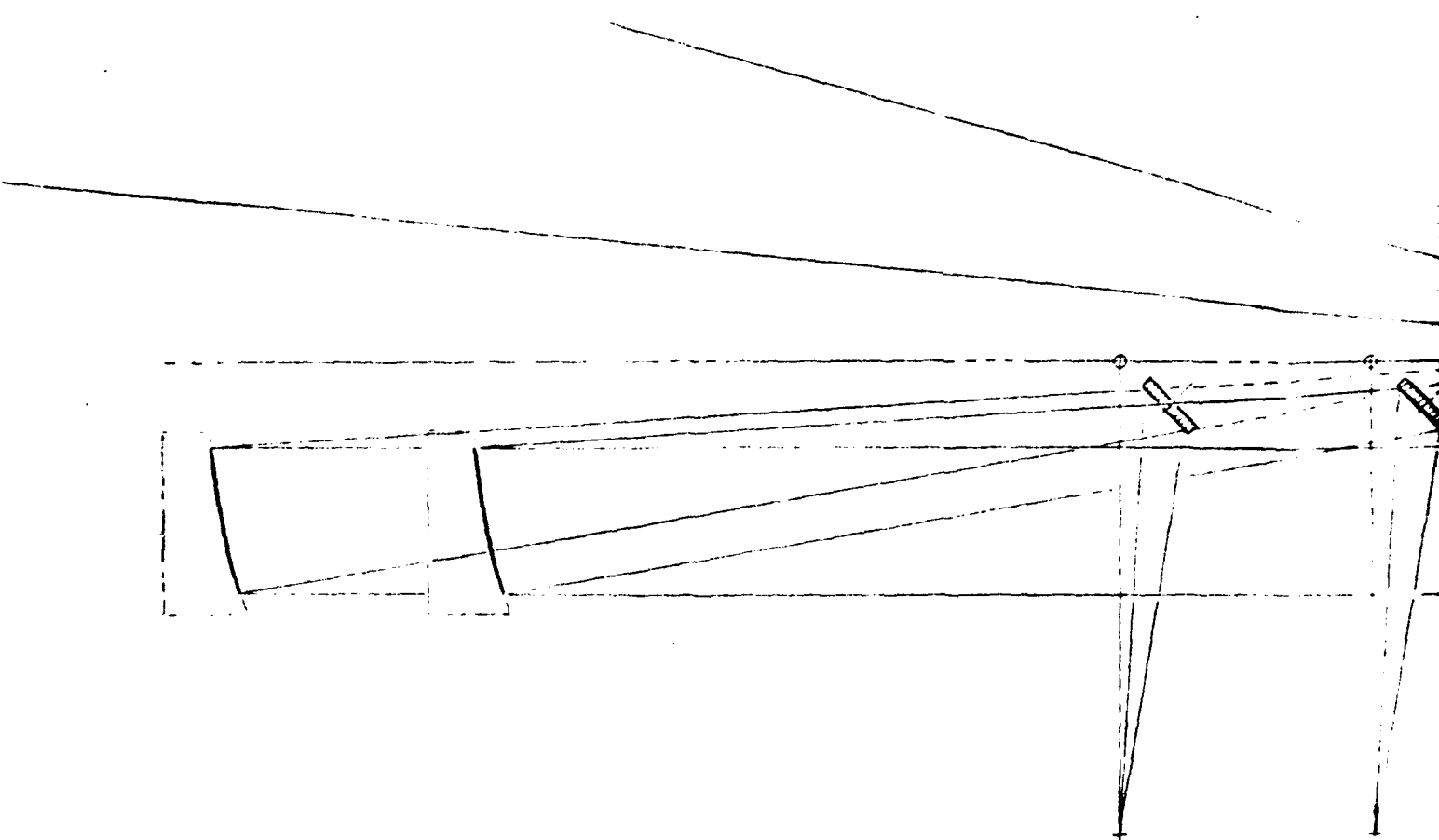
SECTION OF GROOVES
E-10/1

.00
.03

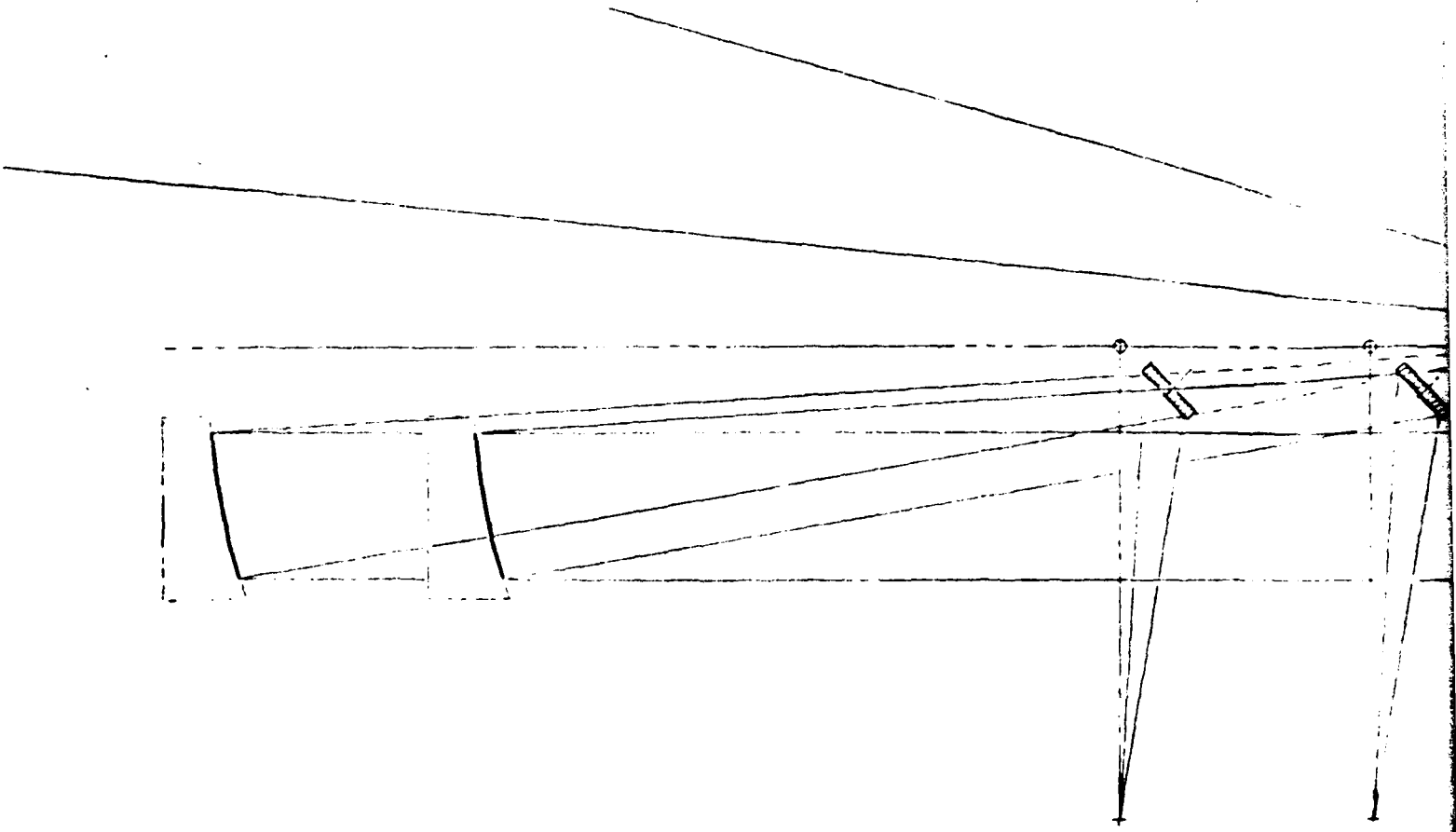
CONFIGURATIONS

PRIMARY, SECONDARY
& TERTIARY MIRRORS HULL & NOTED

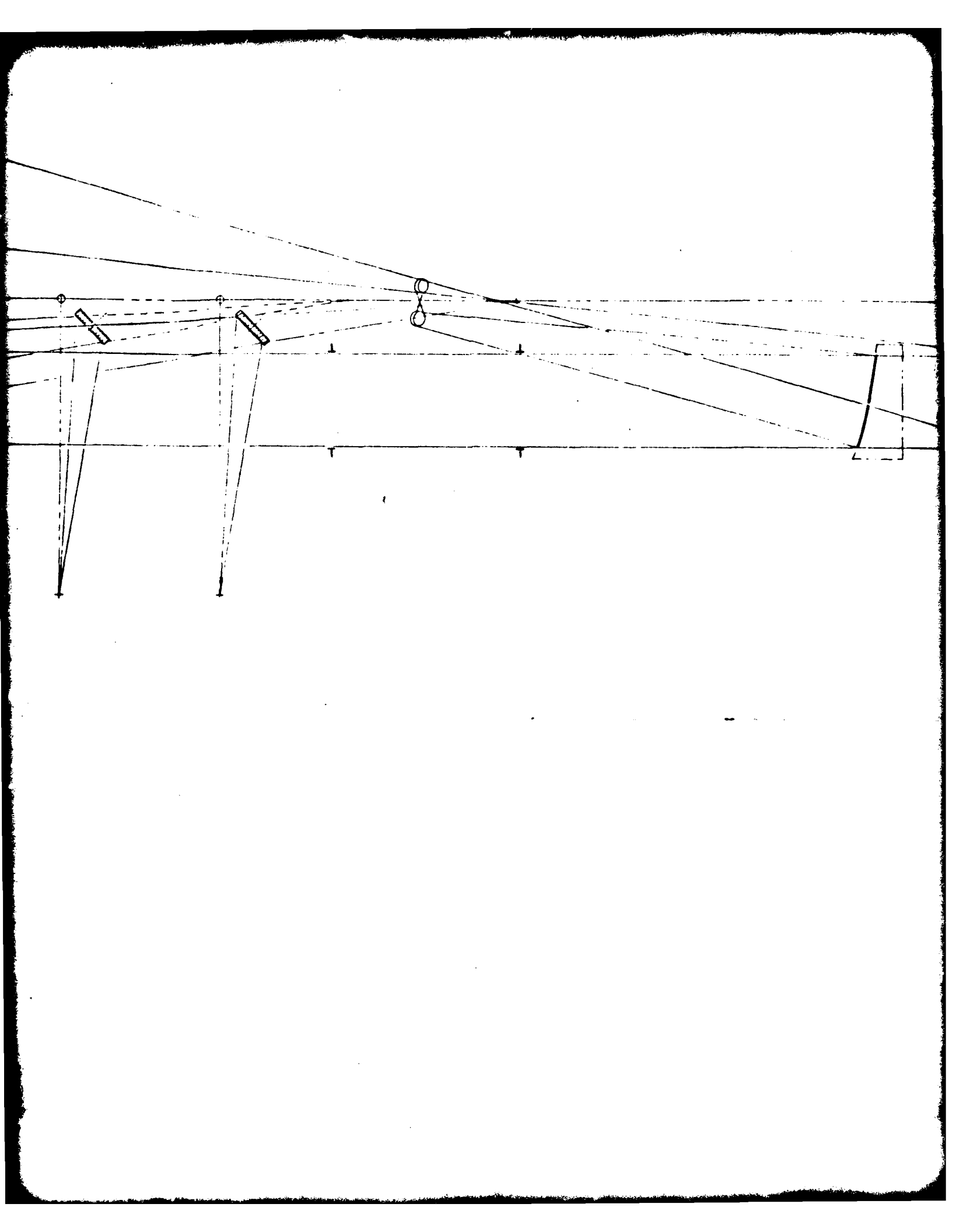
NACOM

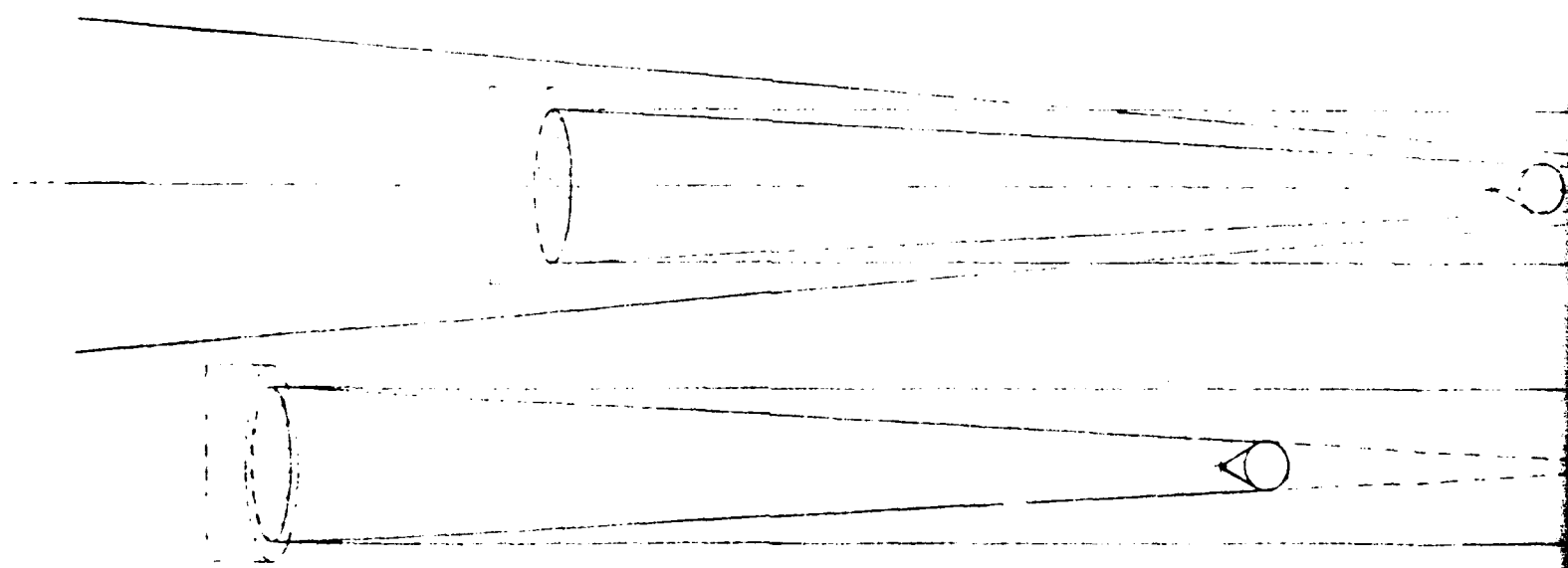


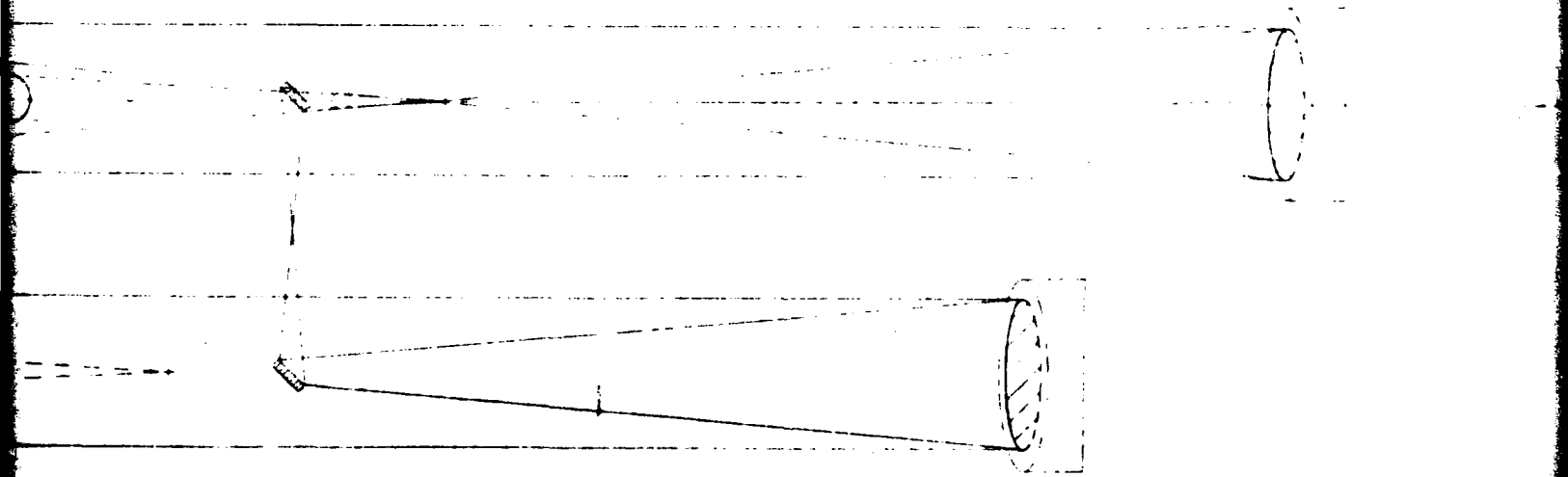
THIS PAGE IS BEST QUALITY PRACTICE
FROM COPY SENT TO DDC

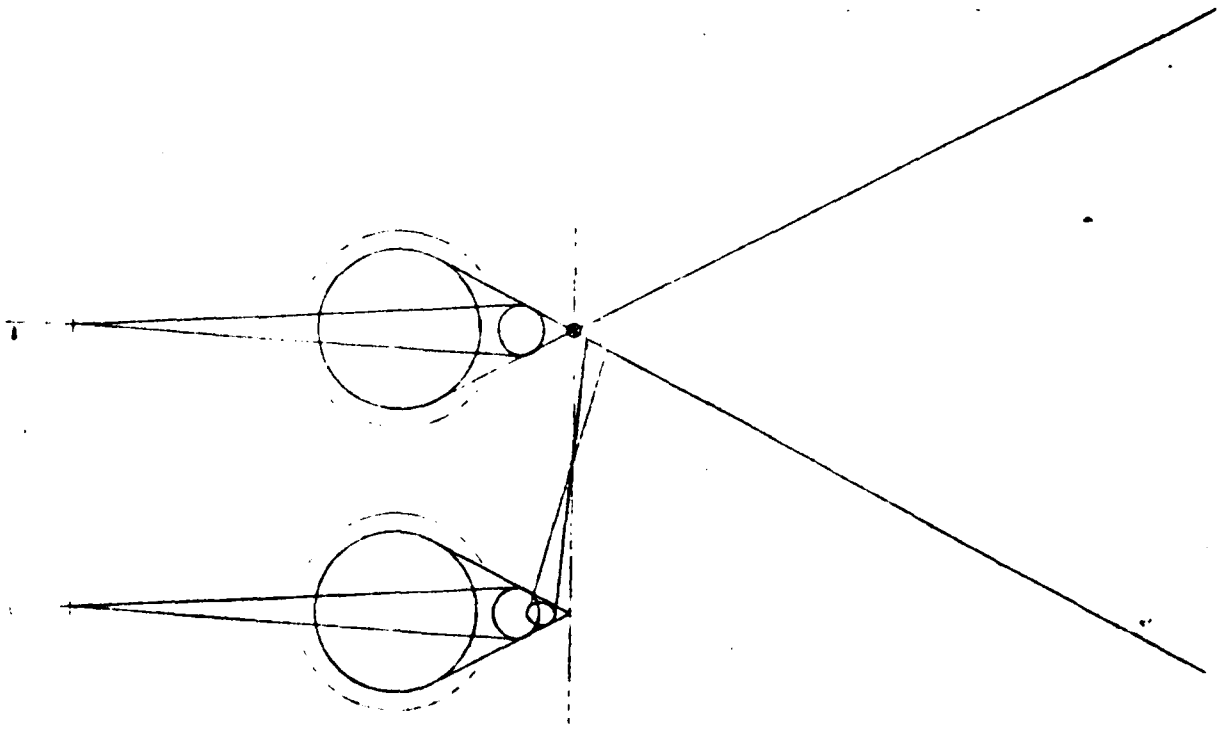


THIS PAGE IS OF LOW QUALITY PRACTICE
FROM COPY FROM THE TO EDC









MILON SECONDARY GEOMETRY
SCALE 1/8
R-0027

APPENDIX A

ACCOS V USER'S MANUAL

(Scientific Calculations, Inc., 1972)

The order in which records are entered for a given surface is, for the most part, arbitrary. The program expects a GRATX or GRATY Record to precede a GORD Record and expects the last record entered for any surface (other than the image surface) to be a GLASS, AIR, REFL, PIKUP GLASS, or [Glass Manufacturer] Record. The image surface data is terminated by an EOS Record.

Dummy planes representing entrance and exit pupils may be inserted after the object surface and preceding the image surface if an ASTOP record has been entered at any surface. If requested to do so, the program will maintain the positions of entrance and/or exit pupil planes so that they coincide with the gaussian images (in the object and image space, respectively) of the ASTOP surface.

Surface Shape Records

The records described in this section define the shape of a surface. Every surface is assumed to have an axis of revolution parallel to one of the three axes of the local coordinate system associated with the surface. Surfaces are classified according to their axis of revolution as indicated below:

(a) Axially Symmetric Surfaces

These surfaces have the Z axis as their axis of revolution and are described by the equation:

$$Z = c\rho^2 / [1 + \sqrt{1 - (\kappa + 1)c^2\rho^2}] + d\rho^4 + e\rho^6 + f\rho^8 + g\rho^{10}$$

where $\rho^2 = x^2 + y^2$

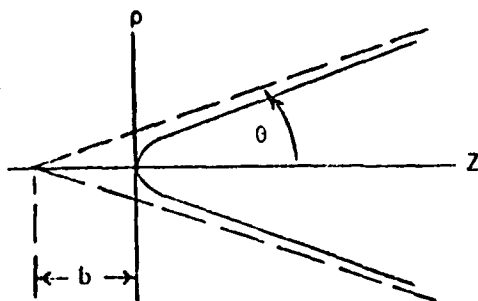
If d , e , f , and g are all zero, the surface is a conic section of revolution and is defined by the equation:

$$Z = c[\rho^2 + (\kappa + 1)Z^2]/2$$

" c " is the vertex curvature and " κ " is called the conic constant. The table below indicates the kind of surface which results from various values of κ :

<u>Range or value of κ</u>	<u>Surface Shape</u>
$\kappa < -1$	Hyperboloid
$\kappa = -1$	Paraboloid
$-1 < \kappa < 0$	Ellipsoid of revolution about major axis
$\kappa = 0$	Sphere
$\kappa > 0$	Ellipsoid of revolution about minor axis

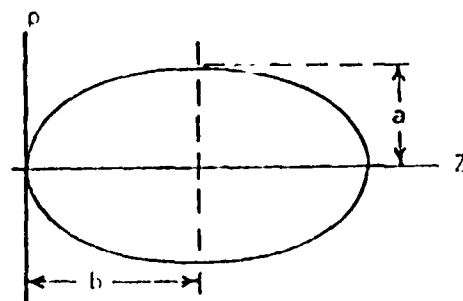
The figures below show geometric parameters a , b , and θ . The way in which c (the vertex curvature) and κ (the conic constant) relate to these parameters is shown by the equations given with the figures.



$$\underline{\kappa < -1}$$

$$\kappa = -(1 + \tan^2 \theta)$$

$$c = 1/[(\kappa + 1)b]$$



$$\underline{\kappa > -1}$$

$$c = (a^2 - b^2)/b^3$$

$$c = 1/[(\kappa + 1)b]$$

Tilt and Decentering Records

The records described in this section permit the location and orientation of a surface to be specified relative to the reference coordinate system established by the preceding surface. Prior to the specification of decenterations and tilt angles it is assumed that the local coordinate system of the surface has its Z axis coincident with that of the reference coordinate system, its X and Y axes respectively parallel to the X and Y axes of the reference system, and its origin at a distance t from the origin of the reference system. The distance t is specified by a "Surface Separation Record" associated with the preceding surface.

The local coordinate system of the current surface becomes the reference coordinate system for the next surface after tilting and/or decentering has been performed.

Tilt and decentering records are not admissable for the object surface, since the local coordinate system of the object surface is the initial reference coordinate system.

"DEC", y_d x_d

In the absence of TILT or RTILT Records, the origin of the local coordinate system of this surface is shifted to $(X, Y, Z) = (x_d, y_d, t)$ in the previous reference coordinate system — i.e., this surface is decentered from the Z axis by x_d in the X direction and y_d in the Y direction.

If a TILT Record is entered, the Euler angle coordinate rotations are made after decentering has been performed in the manner indicated above.

If an RTILT Record is entered, a reversed sequence of Euler angle rotations are made first. Then decenterations $-x_d$ and $-y_d$ are applied in the new coordinate system generated by the rotations.

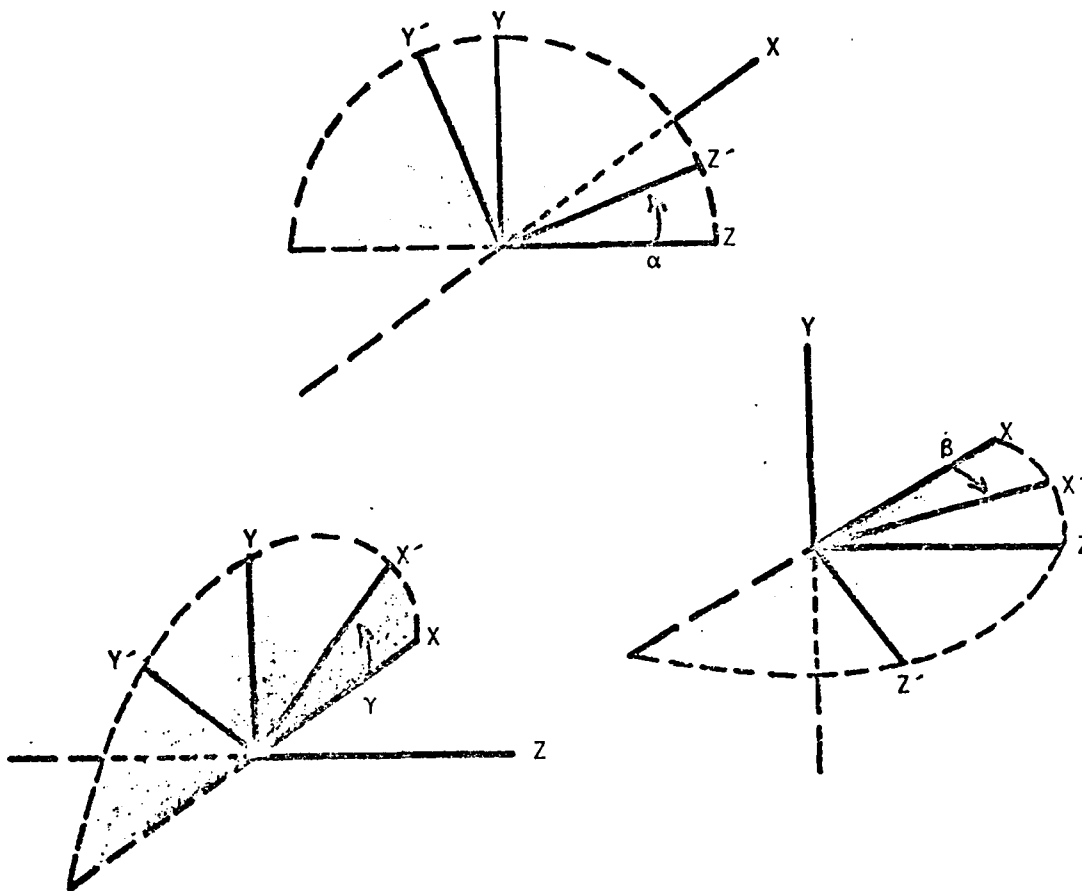
"TILT", α β γ

The local coordinate system of the current surface is tilted by successive Euler angle rotations α , β , and γ . If the surface is decentered, decentering is performed first. α , β , and γ are expressed in degrees.

"RTILT", α β γ

The local coordinate system of the current surface is tilted by successive Euler angle rotations $-\gamma$, $-\beta$ and $-\alpha$. If the surface is decentered, decentering is performed after tilting, and the signs of x_d and y_d are reversed. α , β , and γ are expressed in degrees.

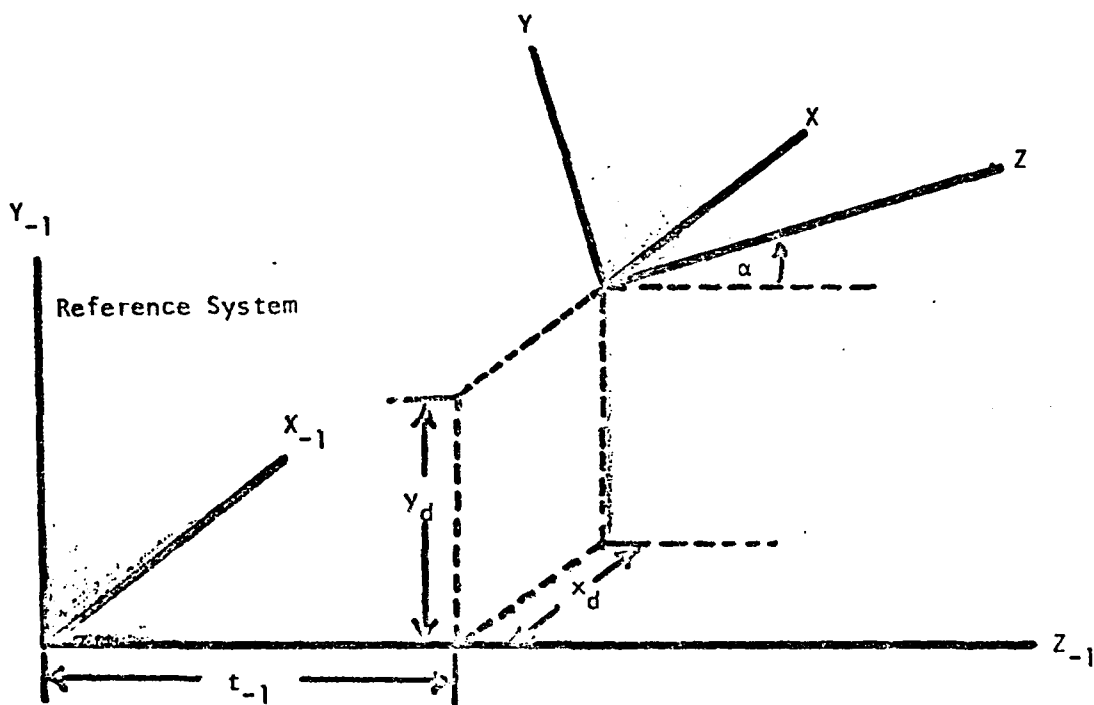
An RTILT Record might typically be used to return to the original coordinate system following the tilting of an element or group of surfaces.



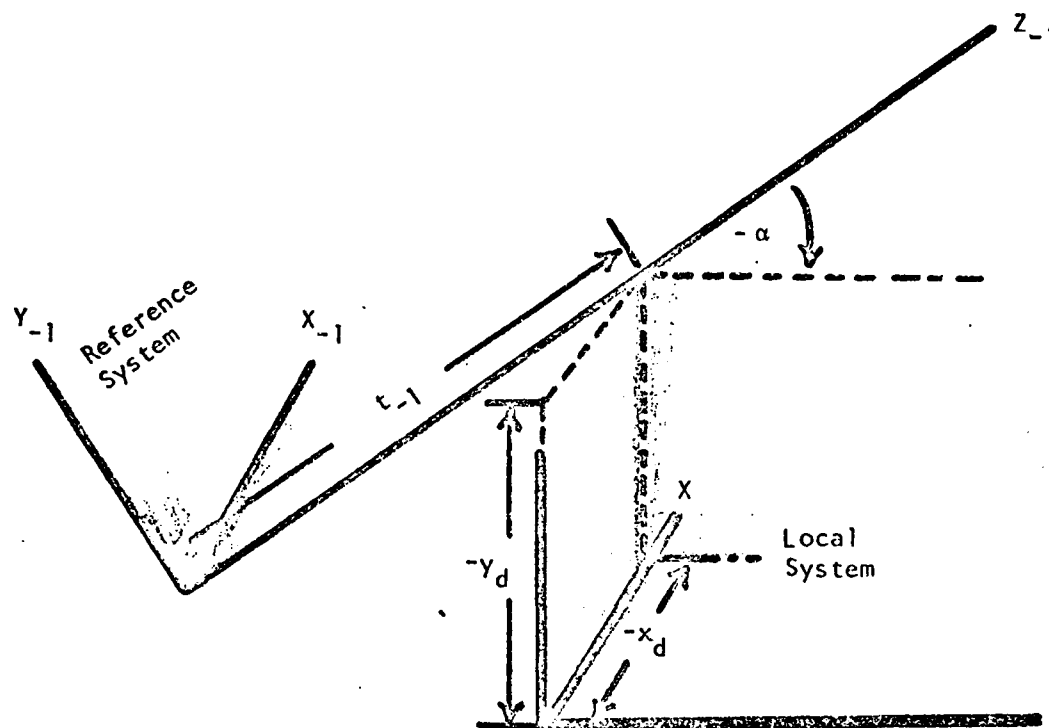
All-Positive Euler Angle Rotations

- For TILT: (1) rotate about X axis through angle α
 (2) rotate about new Y axis through angle β
 (3) rotate about new Z axis through angle γ

- For RTILT: (1) rotate about Z axis through angle $-\gamma$
 (2) rotate about new Y axis through angle $-\beta$
 (3) rotate about new X axis through angle $-\alpha$



TILT (α only) with Decentering



RTILT (α only) with Decentering

The order in which records are entered for a given surface is, for the most part, arbitrary. The program expects a GRATX or GRATY Record to precede a GORD Record and expects the last record entered for any surface (other than the image surface) to be a GLASS, AIR, REFL, PIKUP GLASS, or [Glass Manufacturer] Record. The image surface data is terminated by an EOS Record.

Dummy planes representing entrance and exit pupils may be inserted after the object surface and preceding the image surface if an ASTOP record has been entered at any surface. If requested to do so, the program will maintain the positions of entrance and/or exit pupil planes so that they coincide with the gaussian images (in the object and image space, respectively) of the ASTOP surface.

Surface Shape Records

The records described in this section define the shape of a surface. Every surface is assumed to have an axis of revolution parallel to one of the three axes of the local coordinate system associated with the surface. Surfaces are classified according to their axis of revolution as indicated below:

(a) Axially Symmetric Surfaces

These surfaces have the Z axis as their axis of revolution and are described by the equation:

$$Z = c\rho^2/[1 + \sqrt{1 - (\kappa + 1)c^2\rho^2}] + d\rho^4 + e\rho^6 + f\rho^8 + g\rho^{10}$$

where $\rho^2 = x^2 + y^2$

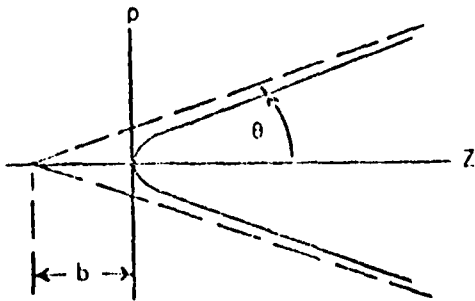
If d, e, f, and g are all zero, the surface is a conic section of revolution and is defined by the equation:

$$Z = c[\rho^2 + (\kappa + 1)Z^2]/2$$

"c" is the vertex curvature and " κ " is called the conic constant. The table below indicates the kind of surface which results from various values of κ :

<u>Range or value of κ</u>	<u>Surface Shape</u>
$\kappa < -1$	Hyperboloid
$\kappa = -1$	Paraboloid
$-1 < \kappa < 0$	Ellipsoid of revolution about major axis
$\kappa = 0$	Sphere
$\kappa > 0$	Ellipsoid of revolution about minor axis

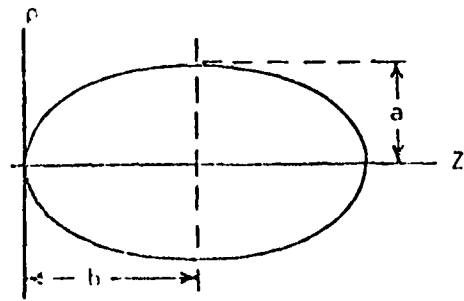
The figures below show geometric parameters a, b, and θ . The way in which c (the vertex curvature) and κ (the conic constant) relate to these parameters is shown by the equations given with the figures.



$$\kappa < -1$$

$$\kappa = -(1 + \tan^2 \theta)$$

$$c = 1/[(\kappa + 1)b]$$



$$\kappa < -1$$

$$\kappa = (a^2 - b^2)/b^2$$

$$c = 1/[(\kappa + 1)b]$$

Tilt and Decentering Records

The records described in this section permit the location and orientation of a surface to be specified relative to the reference coordinate system established by the preceding surface. Prior to the specification of decentrations and tilt angles it is assumed that the local coordinate system of the surface has its Z axis coincident with that of the reference coordinate system, its X and Y axes respectively parallel to the X and Y axes of the reference system, and its origin at a distance t from the origin of the reference system. The distance t is specified by a "Surface Separation Record" associated with the preceding surface.

The local coordinate system of the current surface becomes the reference coordinate system for the next surface after tilting and/or decentering has been performed.

Tilt and decentering records are not admissible for the object surface, since the local coordinate system of the object surface is the initial reference coordinate system.

"DEC", y_d x_d

In the absence of TILT or RTILT Records, the origin of the local coordinate system of this surface is shifted to $(X, Y, Z) = (x_d, y_d, t)$ in the previous reference coordinate system — i.e., this surface is decentered from the Z axis by x_d in the X direction and y_d in the Y direction.

If a TILT Record is entered, the Euler angle coordinate rotations are made after decentering has been performed in the manner indicated above.

If an RTILT Record is entered, a reversed sequence of Euler angle rotations are made first. Then decentrations $-x_d$ and $-y_d$ are applied in the new coordinate system generated by the rotations.

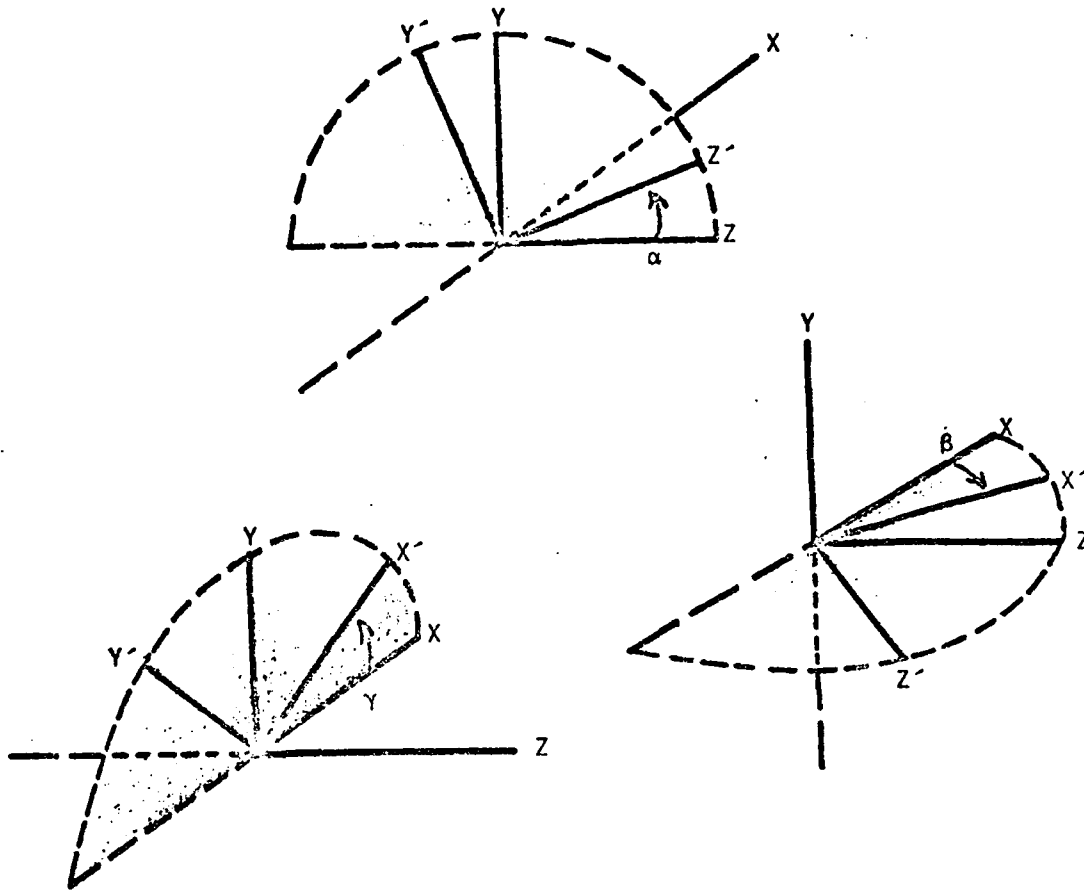
"TILT", α β γ

The local coordinate system of the current surface is tilted by successive Euler angle rotations α , β , and γ . If the surface is decentered, decentering is performed first. α , β , and γ are expressed in degrees.

"RTILT", α β γ

The local coordinate system of the current surface is tilted by successive Euler angle rotations $-\gamma$, $-\beta$ and $-\alpha$. If the surface is decentered, decentering is performed after tilting, and the signs of x_d and y_d are reversed. α , β , and γ are expressed in degrees.

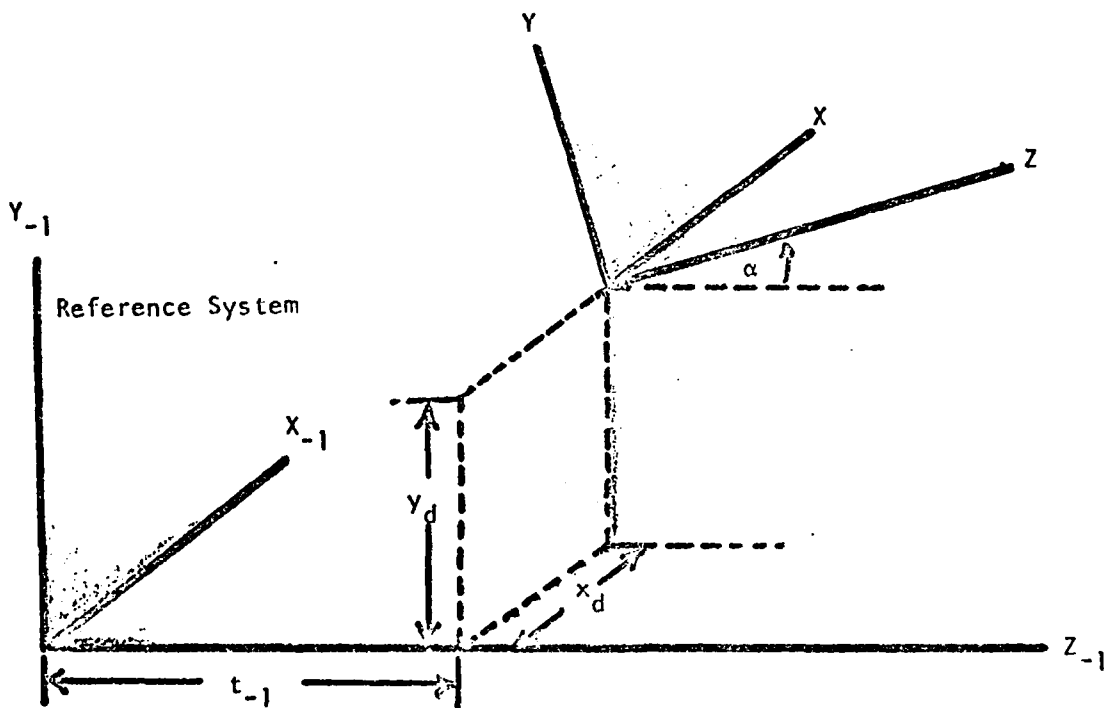
An RTILT Record might typically be used to return to the original coordinate system following the tilting of an element or group of surfaces.



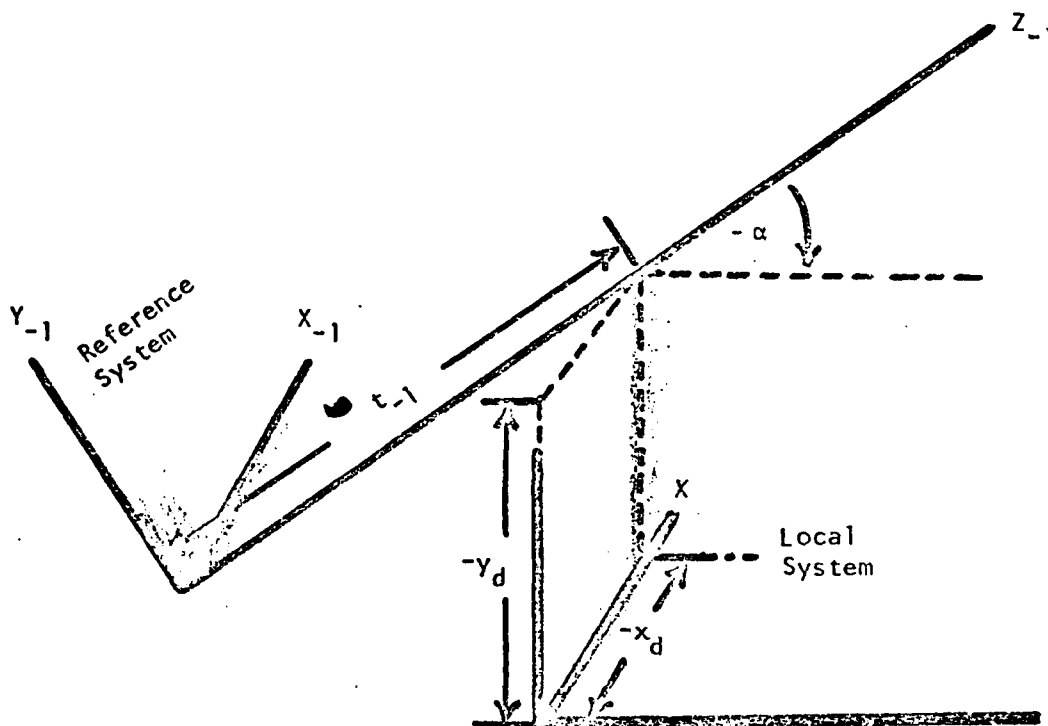
All-Positive Euler Angle Rotations

- For TILT: (1) rotate about X axis through angle α
 (2) rotate about new Y axis through angle β
 (3) rotate about new Z axis through angle γ

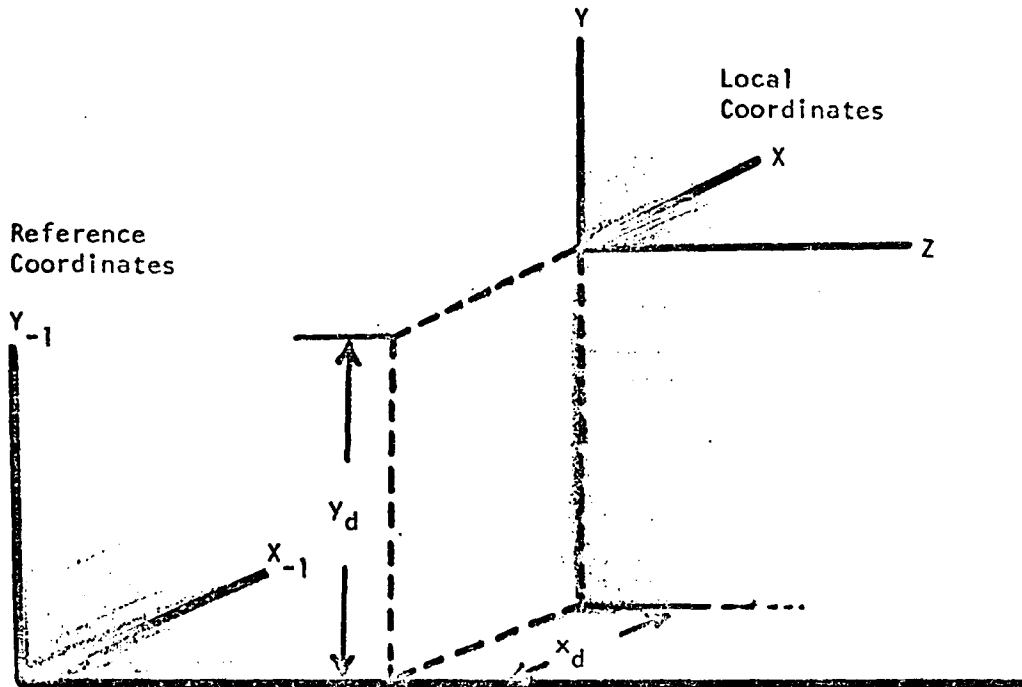
- For RTILT: (1) rotate about Z axis through angle $-\gamma$
 (2) rotate about new Y axis through angle $-\beta$
 (3) rotate about new X axis through angle $-\alpha$



TILT (α only) with Decentering



RTILT (α only) with Decentering



DECEN Only

APPENDIX B

COMPUTER REDUCTION OF 82-IN. MIRROR

503.720	500.550	501.424	501.424	502.320	503.154	503.908
503.024	END					
498.125	498.976	499.824	500.612	501.428	501.428	502.304
504.034	504.941	505.836	506.158	506.551	END	
507.247	498.024	498.869	499.664	500.497	501.215	501.245
503.117	504.025	504.916	505.807	506.474	507.117	507.543
END						
495.400	497.244	497.942	498.645	499.490	500.350	501.080
501.934	502.919	503.828	504.841	505.730	506.724	507.459
504.448	END					
495.544	496.308	497.089	497.786	498.604	499.333	500.087
500.892	501.745	502.672	503.629	504.582	505.672	506.661
505.372	508.810	END				
495.442	496.235	496.974	497.699	498.416	499.098	499.927
500.602	501.515	502.408	503.426	504.409	505.314	506.344
504.410	508.938	509.264	END			
495.521	495.362	496.164	496.869	497.524	498.310	498.960
500.450	501.204	502.125	503.067	504.117	505.402	
507.612	508.524	509.241	509.550	END		
495.495	495.300	496.034	496.805	497.471	498.258	498.922
500.271	500.271	500.910	501.723	502.852	503.937	505.254
507.618	505.620	509.344	509.722	END		
495.642	497.410	496.039	496.786	497.440	498.176	498.825
500.103	500.103	500.849	501.306	502.510	503.834	505.205
507.621	508.751	509.431	509.818	END		
494.552	495.332	495.994	496.631	497.436	498.011	498.770
500.078	500.008	500.591	501.053	502.254	503.848	505.234
507.770	508.750	509.476	509.933	END		
495.539	495.343	496.039	496.677	497.419	498.076	498.820
500.075	500.075	500.597	501.469	502.435	504.020	505.337
507.755	508.817	509.540	509.846	END		
494.452	495.225	495.939	496.703	497.483	498.143	498.811
500.219	500.219	501.917	501.918	502.990	504.200	505.446
507.497	508.378	509.510	509.749	END		
495.272	496.069	496.826	497.550	498.294	499.043	499.792
500.474	501.471	502.438	503.460	504.505	505.630	506.860
503.943	509.339	END				
495.379	496.126	496.873	497.734	498.480	499.201	500.019
500.535	501.855	502.661	503.643	504.724	505.813	507.021
505.833	509.234	END				
495.207	496.474	497.793	498.620	499.455	500.314	501.097
502.047	503.012	503.916	505.053	506.060	507.178	508.062
505.924	END					
497.054	497.900	498.728	499.571	500.443	501.145	501.165

502.212	503.159	504.163	505.189	506.206	507.209	507.926	508.267
END							
494.059							
495.452	494.031	498.904	499.785	500.571	501.511	501.511	502.458
503.259	504.520	505.351	506.196	507.121	507.436	END	
493.239							
497.577	498.953	499.807	500.714	501.587	501.587	502.548	503.502
502.359	505.275	506.002	506.413	END			
494.572	500.619	501.491	501.491	502.388	503.224	504.145	504.682
END							
DCNE							

OSK 02/20/76 15.56.59.

OSK-02 INCH #1 2/19/76
SURFACE DEVIATION MEASURED IN WAVELENGTHS OF .633 MICRONS
TILT AND DEFOCUS MEASURED FROM DIFFRACTION FOCUS

N RMS
0 2.528
1 .276
2 .193
3 .069
4 .032
5
6
7
8
9
10
11
12
13
14
15
16
17
18
19
20
21
22
23
24
25
26
27
28
29
30
31
32
33
34
35
36

FIRST ORDER (GAUSS) DESCRIPTION

MAGNITUDE ANGLE DESIGNATION
TILTS DEG
5.905 1.2 TILT
-0.554 DEFOCUS

STREHL RATIO .003

THIRD ORDER (SEIDEL) ABERRATIONS

MAGNITUDE ANGLE DESIGNATION
TILTS DEG
4.320 .9 TILT
-0.570 DEFOCUS
1.300 ASTIGMATISM
-1.103 COMA
2.347 3RD-ORDER SPHERICAL ABERRATION

FOLLOWING THIRD ORDER TERMS WERE SUBTRACTED-

RESIDUAL SURFACE VARIATIONS
RMS .193 MAX .720 MIN -.275 SPAN .994
MEAN -.002
STREHL RATIO .003

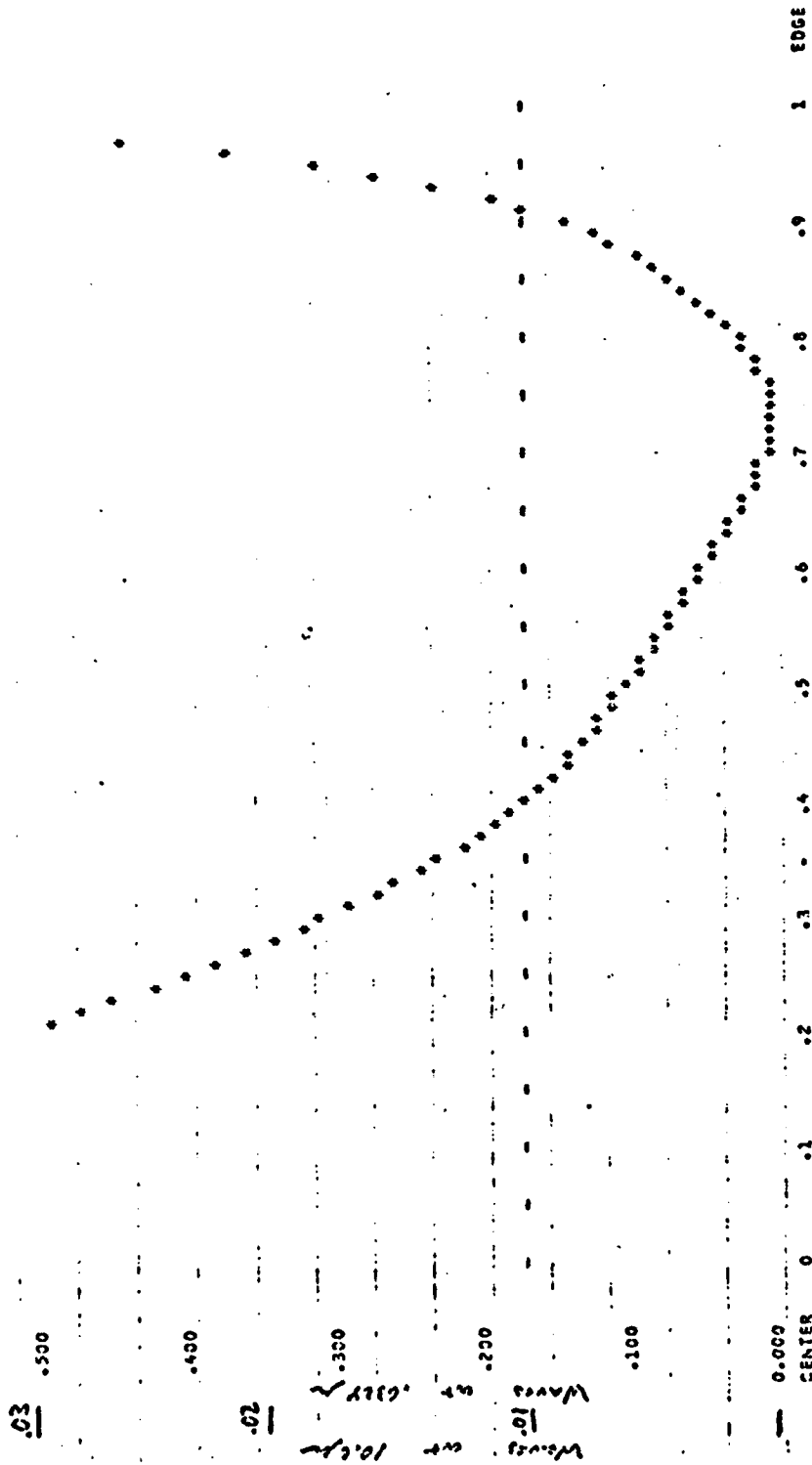
OSK 02/20/76 15.57.06.

STEP .10 RMS .199 MAX .891 MIN -.267 SPAN 1.147
 AV -.001 2/19/76



DSK 02/20/76 15:57.19.

.01000 1.5 INCH #1 2/19/76
 AVERAGE RADIAL PROFILE
 .AV RMS MAX MIN SPAN
 .000 .168 .624 -.166 .790



0.000 CENTER 0

.1

.2

.3

.4

.5

.6

.7

.8

.9

1

EDGE